Title: Altered Prostasin (CAP1/Prss8) Expression Favors Inflammation and Tissue Remodeling in DSS-induced Colitis.

Authors: Keppner A, Malsure S, Nobile A, Auberson M, Bonny O, Hummler E

Journal: Inflammatory bowel diseases

Year: 2016 Dec

Volume: 22

Issue: 12

Pages: 2824-2839

DOI: 10.1097/MIB.0000000000000940

"Altered prostasin (CAP1/Prss8) expression favours inflammation and tissue remodelling in DSS-induced colitis"

Anna Keppner, PhD, [1] Sumedha Malsure, PhD, [1,3] Antoine Nobile, MD, [2] Muriel Auberson, PhD, [1] Olivier Bonny, MD PhD, [1] Edith Hummler, PhD, [1]

[1] Département de Pharmacologie & de Toxicologie, University of Lausanne, Lausanne, Switzerland

[2] Institut Universitaire de Pathologie, University Hospital of Lausanne (CHUV), Lausanne, Switzerland

Running head: prostasin protects against DSS-induced colitis

Grant number and source of support: This work was supported by the Swiss National Science Foundation (Grant 31003A_127147/1 and 31003A_144198/1 to E.Hummler).

Financial disclosure: The authors have no conflicts of interest to disclose.

Current address:

[3] Elanco Animal Health, Basel, Switzerland

Corresponding author:

Edith Hummler, University of Lausanne, Department of Pharmacology and Toxicology, Rue du Bugnon 27, CH-1011 Lausanne, Switzerland. Tel. +41/21-692 5357, Fax. +41/21-692 5355. e-mail: Edith.Hummler@unil.ch

Abstract

Background: Inflammatory bowel diseases (IBD) including ulcerative colitis and Crohn's disease are diseases with impaired epithelial barrier function. We aimed to investigate whether mutated prostasin and thus, reduced colonic epithelial sodium channel (ENaC) activity predispose to develop an experimentally dextran sodium sulfate (DSS)-induced colitis.

Methods: Wildtype, heterozygous (fr^{CR}/+) and homozygous (fr^{CR}/fr^{CR}) prostasin mutant rats were treated 7 days with DSS and 7 days of recovery and analysed with respect to histology, clinicopathological parameters, inflammatory marker mRNA transcript expression, and sodium transporter protein expression.

Results: In this study, a more detailed analysis on rat fr^{CR}/fr^{CR} colons revealed reduced number of crypt and goblet cells, and local angiodysplasia, as compared to heterozygous (fr^{CR}/+) and wildtype littermates. Following 2% DSS treatment for 7 days followed by 7 days recovery, fr^{CR}/fr^{CR} animals lost body weight, and reached maximal diarrhea score and highest disease activity after only 3 days, and strongly increased cytokine levels. The histology score significantly increased in all groups, but fr^{CR}/fr^{CR} colons further displayed pronounced histological alterations with near absence of goblet cells, rearrangement of the lamina propria and presence of neutrophils, eosinophils, and macrophages. Additionally, fr^{CR}/fr^{CR} colons showed ulcerations and edemas, that were absent in fr^{CR}/+ and wildtype littermates. Following recovery, fr^{CR}/fr^{CR} rats reached, although significantly delayed, near-normal diarrhea score and disease activity, but exhibited severe architectural remodelling, despite unchanged sodium transporter protein expression.

Conclusions: In summary, our results demonstrate a protective role of colonic prostasin expression against experimental colitis, and thus represents a susceptibility gene in the development of IBD.

Keywords: prostasin, dextran sodium sulfate, inflammatory bowel disease

Introduction

Crohn's disease (CD) and ulcerative colitis (UC) are inflammatory diseases with chronic defects of the gastrointestinal tract, leading to severe bloody diarrhea, abdominal pain and rectal bleeding in patients affected by this class of disorders.[1] While the understanding of the structural changes associated with inflammatory bowel diseases (IBD) have progressed, the molecular basis and pathways implicated in the disease remain largely unknown. The intestinal mucosa plays a crucial role in the transport of molecules across the epithelium as well as in the immune protection of the intestinal tract by participating in the coordinated communication between the external environment and the immune system.[2] When inflamed after epithelial injury, the mucosa loses its barrier function, leading to water loss in the stool, and to impaired ionic and molecular transport. Inflammation of the intestinal tract and chronic colitis can be induced by chemical compounds like e.g., the administration of Dextran sodium sulfate (DSS).[3-5] Various animal models of chronic colitis show increased permeability of the intestinal mucosa, likely because of epithelial damage and tight junction injury.[6,7] DSS treatment itself of BALB/c mice leads to the loss of the tight junction protein ZO-1 and increased epithelial permeability.[7]

In patients, increased colonic epithelial permeability was reported that preceded the onset of IBD.[8-10] Indeed, an increasing number of genes are linked to intestinal permeability, immunity, protection from pathogens and solute transport, like e.g. claudins,[11] tumor necrosis factor α (TNFα),[12] interleukins,[13] or the epithelial sodium channel (ENaC)[14] and thus as associated with IBD, either as susceptibility genes or through their protective role. Indeed, in colonic epithelial preparations from UC patients, decreased electrogenic sodium transport was measured as compared to colonic preparations from healthy patients, most likely through

reduced β- and γ-ENaC mRNA transcript expression levels.[14] Pre-incubation of rat colonic epithelial preparations with either TNFα or IL-1β decreases ENaC-mediated electrogenic sodium transport and inhibits the transcription of β- and γ-ENaC.[11,15]

The membrane-bound serine protease prostasin (CAP1/Prss8) was previously identified as a channel activating protease (CAP), since it increases ENaC-mediated sodium currents by increasing the open probability (P_O) of single channels when co-expressed in the *Xenopus* oocyte expression system.[16-18] *In vivo*, prostasin mutations result in embryonic lethality[19,20] or reduced embryonic viability, skin defects (including epidermal barrier impairment, leading to early postnatal lethality due to severe skin dehydration as a consequence of tight junction defects)[19,21] and decreased ENaC activity as measured in colon.[21] ENaC therefore determines the body sodium homeostasis.[22] As a consequence of the reduced epithelial sodium transport in adulthood, the resolution of pulmonary edema in cases of lung injury is significantly delayed,[23] while in colon, animals develop a salt-losing syndrome with mineralocorticoid resistance.[24]

We previously reported in the fr^{CR} rat model, that harbors a 16 base pairs in-frame deletion in the prostasin gene resulting in a G54-P57 deletion in the prostasin protein,[25,26] decreased protease activity along with increased water loss through the skin and the presence of mild diarrhea,[21] suggesting an impaired barrier function in the colon[8] and decreased ENaC activity.

In the present study, we aimed to investigate whether reduced prostasin activity and/or reduced ENaC expression predispose to experimentally-induced colitis, and the implication of prostasin in maintaining the intestinal barrier function. Our results demonstrate that intestinal prostasin (CAP1/Prss8) (i) preserves the colonic integrity, (ii) protects against DSS-induced inflammation, and (iii) likely protects against tissue remodeling.

Material and methods

Animals

Age-matched 3 months old +/+ (wild-type), fr^{CR}/+ (heterozygous), and fr^{CR}/fr^{CR} (homozygous mutant) male and female littermates were used for all experiments. Genotyping was performed as previously described.[26]

The animals were housed in a temperature- and 60% humidity-controlled environment with a 12h light/dark cycle, and had free access to food and water if not under experimentation. All experiments were approved by Swiss federal guidelines and local authorities.

Induction of Colitis

Colitis was induced as previously described.[3,6,27,] Briefly, a 2% (m/v) solution of dextran sodium sulfate (Mol.wt. 36000-50000, MP Biologicals, LLC, Illkirch Cedex, France) in tap water was daily prepared and administered *ad libitum* during 7 days, followed by 7 days of recovery with normal drinking water. During the 14 days of experimentation, body weight, diarrhea, and presence of occult blood in the feces (Guaiac test, HEMDETECT, DIPROmed GmbH, Weigelsdorf, Austria) were daily assessed. The attributed score for diarrhea was : 0, no diarrhea ; 1, mild diarrhea ; 2, severe diarrhea ; 3, mild diarrhea with blood ; 4, severe diarrhea with blood. The animals were sacrificed at the end of the experiment, and colon length was measured (anus to caecum). The disease activity index was calculated as previously described.[27]

Histological Analysis

Distal colons were fixed in 4% paraformaldehyde and further processed for paraffin embedding. 3μm sagittal sections were cut and dried 15 minutes at 60°C. The paraffin was removed and the slides re-hydrated as following : Xylol 2x5 min., ethanol 100% 2x1 min., ethanol 95% 1 min., and water. The H&E staining was performed as follows : Glychemalun

126 solution (Hematein 0.013M, Gurr #34036 ; potassium alum 0.3133M, Merck #1047 ; glycerol
127 30% ; acetic acid 1%, Merck #1.00063) for 4 minutes, tap water with acid alcohol 1% for 3
128 seconds, tap water for 15 seconds, water plus few drops of NH_3 together with tap water,
129 erythrosine solution 0.2% (Erythrosin 0.0023M, Merck #15936 ; formol 0.1%, Merck #4003)
130 for 30 seconds, and tap water. Alcian blue (AB) staining was performed as follows : alcian
131 blue (DIAPATH C0052) for 20 minutes, tap water, nuclear stain for 3 minutes (Waldeck, 2E-
132 01), and water. Slides were dehydrated by following steps ethanol 70% to xylol and mounted
133 (Eukitt, Hatfield, PA). Pictures were taken using an Axion HRC (Carl Zeiss MicroImaging
134 Inc.). The histology score to quantify the degree of intestinal inflammation was calculated as
135 previously described.[28] The score was attributed as shown in **table 1**.
136
137 *RNA Extraction and qRT-PCR*
138 Colons were frozen in liquid nitrogen and stored at -80°C. Tissues were homogenized using
139 TissueLyser (Qiagen, Valencia, CA), and mRNA was isolated using the Qiagen RNeasy Mini
140 Kit (Basel, Switzerland) according to the manufacturer's instructions. cDNA synthesis was
141 performed using 1.5µg of mRNA which was reverse transcribed using PrimeScript RT
142 reagent kit according to the manufacturer's instructions (Takara Bio Inc Japan). Real-time
143 PCR was performed using Power SYBRgreen PCR Master Mix (Applied Biosystems) and
144 run using Applied Biosystems 7500 Fast (Carlsbad, CA). Each measurement was performed
145 as duplicate. Quantification of fluorescence was normalized to *Gapdh*. Primers for *IL-6,*
146 *TNFα, TGFβ1, PAR2, iNOS*, and *Gapdh* were previously described.[29-32] The sequences of the
147 primers used were the following: *IL-1β_F*: 5'-CCT TGT GCA AGT GTC TGA AGC-3', *IL-*
148 *1β_R*: 5'-TCA GAC AGC ACG AGG CAT TT-3' ; *IL-10_F* : 5'-GTT GCC AAG CCT TGT
149 CAG AAA-3', *IL-10_R* : 5'-TTT CTG GGC CAT GGT TCT CT-3' ; *IL-12_F* : 5'-CCG GTC
150 CAG CAT GTG TCA AT-3', *IL-12_R* : 5'-CAC TTG GCA GGT CCA GAG AC-3' ; *IL-*

18_F : 5'-ACC GCA GTA ATA CGG AGC AT-3', *IL-18_R* : 5'-CGT TGG CTG TTC GGT CGA TA-3' ; *matriptase_F* : 5'-ACA GTC CCT ACC CAG CTC AT-3', *matriptase_R* : 5'-GCA GAA CTT CTC CCC GTT GA-3' ; *MMP3_F* : 5'-CTG CGG GGA GAA GTC TTG TT-3', *MMP3_R* : 5'-TGT TGG ATG GAA GAG ACG GC-3' ; *CXCL2_F* : 5'-GCG CCC AGA CAG AAG TCA TA-3', *CXCL2_R* : 5'-CAG GTA CGA TCC AGG CTT CC-3'.

Protein extraction, SDS-PAGE and Western blot analysis

Colons were subjected to homogenization as previously described,[33,34] in 1ml RIPA buffer (Tris pH 7.2 50mM, NaCl 150mM, NP40 1%, SDS 0.1%, Na-deoxycholate 0.5%, protease inhibitors 1mM [aprotinin + leupeptin + pepstatin, Complete Mini, Roche], PMSF 1mM) using TissueLyser (Qiagen). After 15 minutes centrifugation at 13000 rpm at 4°C, the supernatant was recovered and analyzed for protein content by Bradford assay, and pellet containing muscle tissue was discarded. 30µg of proteins were separated by SDS-PAGE on 10% acrylamide gels, and proteins were electrically transferred to PolyScreen PVDF hybridization transfer membranes (Perkin Elmer, Boston, MA). Membranes were incubated overnight at 4°C with primary rat antibody for α-ENaC (1:500), β- and γ-ENaC (1:1000),[35] NHE1 (1:500) and NHE3 (1:10) (kindly provided by Dr. Daniel Fuster, University of Bern, Switzerland), Na^+, K^+-ATPase (1:10000),[36] occludin (1:1000, Invitrogen 71-1500), claudin-1 (1:1000, Invitrogen 71-7800), ZO-1 (1:1000, Invitrogen 61-7300) and β-actin (1:1000, Sigma-Aldrich) and for 1 hour with donkey anti-rabbit IgG HRP-conjugated secondary antibody (1:10000, Amersham, Burkinghampshire, UK) (all antibodies in TBS-Tween 1% and dried milk 2%). The signal was revealed using SuperSignal West Dura detection system (Pierce, Rockford, IL) and quantified using ImageStudio™ Lite program (LI-COR). Kidney extracts from inducible renal-tubule specific Scnn1a KO mice,[37] generated by interbreeding of

Scnn1a$^{lox/lox}$ mice[38] and Pax8::rtTA;TRE::LC1 mice,[39] were used as negative controls for Scnn1a. The same strategy was used for Scnn1b and Scnn1g negative controls.[40]

Transepithelial measurements

Colon preparations were prepared as previously described.[41] Briefly, proximal and distal colon were dissected and opened longitudinally along the mesenteric border. The outer smooth muscle layer was carefully removed with fine forceps and the colon preparation was mounted in Ussing chamber (0.3-cm^2 surface area) bathed in standard Ringer solution (in mM: NaCl 119, $NaHCO_3$ 21, $CaCl_2$ 1.2, $MgCl_2$ 1.2, KH_2PO_4 0.6, K_2HPO_4 24, D-glucose 10) at 37°C and gassed with 95% O_2 and 5% CO_2 to maintain the pH at 7.4. The short circuit current (Isc, in μA) were measured using a computer-controlled voltage-clamp apparatus (VCC-600, Physiological Instruments, San Diego, CA). The transepithelial resistance (R, in Ω*cm^2) were calculated according to Ohm's law from 10 μA pulses of 20 ms duration. Amiloride-sensitive currents were obtained by adding 10 μM amiloride to the mucosal side.

Statistical analysis

Results are presented as mean ± SEM. Throughout the study, and if not otherwise stated, data were analyzed by one-way ANOVA using GraphPad Prism. $P< 0.05$ was considered statistically significant.

Results

fr^{CR}/fr^{CR} rats exhibit altered colon histology and increased levels of inflammatory markers without treatment

In the present study, a detailed histopathological analysis of the colon in untreated *fr^{CR}/ fr^{CR}* animals with reduced colonic prostasin and ENaC activity further revealed presence of local

inflammation and angiodysplasia (**Fig. 1)** and a generally decreased number of goblet and crypt cells, as quantified by Alcian blue (AB) staining (**Fig. 2A,B**), and confirmed by periodic acid-Shiff (PAS) staining (data not shown). No histological alterations were observed in heterozygous animals (**Fig. 1**). The histology score to quantify the degree of intestinal inflammation was, however, not significantly different in the fr^{CR}/fr^{CR} mutant rats as compared to fr^{CR}/fr^{+} and wildtype controls (**Fig. 3A**).

At the mRNA transcript expression level, the protease activated receptor 2 (*PAR2*), tumor growth factor β1 (*TGFβ1*) and matrix metalloprotease 3 (MMP3) were significantly reduced (**Fig. 4B,I,K**), while inducible nitric oxide synthase (*iNOS*) appeared 4-fold increased as compared to wildtype animals (**Fig. 4C**), although no leucocyte and macrophage infiltrations were observable (**Fig. 1**). No differences could be detected for tumor necrosis factor α (*TNFα*), interleukin 1β (*IL-1β*), interleukin 6 (*IL-6*), interleukin 10 (*IL-10*), interleukin 12 (*IL-12*), interleukin 18 (*IL-18*), matriptase, and chemokine (C-X-C motif) ligand 2 (*CXCL2*) (**Fig. 4A,D-H,J,L**). Heterozygous mutant ($fr^{CR}/+$) rats showed intermediate mRNA transcript expression levels for these inflammation markers, being not significantly different from wildtype or homozygous mutant (fr^{CR}/fr^{CR}) rats (**Fig. 4A-L**). In summary, untreated homozygous fr^{CR}/fr^{CR} animals exhibited lower number of crypt and goblet cells and showed increased expression of *iNOS*, although the histology score to quantify intestinal inflammation was not significantly different among the groups.

Untreated fr^{CR}/fr^{CR} rats display reduced NHE1 and NHE3 protein levels, but normal colonic permeability

We investigated whether impaired colonic permeability might underlie the basal diarrhea and the observed histological changes. We analysed the protein expression levels of tight junction proteins in untreated animals. The protein levels of zona occludens 1 (ZO-1), occludin and

claudin-1 were not significantly changed between wildtype, heterozygous mutant (fr^{CR}/+) and homozygous mutants (fr^{CR}/fr^{CR}) (**Fig. 5A-D**). The transepidermal short circuit current (I_{sc}) and the transepidermal resistance (TER) in untreated animals were not significantly different between the genotypes (**Fig. 5H,I**). The diarrhea score in homozygous mutant (fr^{CR}/fr^{CR}) rats was however significantly increased as compared to both wildtype and heterozygous (fr^{CR}/+) rats (**Fig. 5J**). We next analysed the protein levels of the sodium-hydrogen exchangers 1 and 3 (NHE1 and NHE3) and the Na^+,K^+-ATPase in the colon of untreated animals. The protein expression levels of both NHE1 and NHE3 appeared significantly decreased in homozygous (fr^{CR}/fr^{CR}) mutants as compared to wildtype (**Fig. 6A-C**). The protein level of the Na^+,K^+-ATPase was not changed between the genotypes (**Fig. 6A,D**). The protein expression levels of the full-length α-, β-, and γ-ENaC subunits (**Fig. 7A,B,D,E**), and the cleaved α- and γ-ENaC fragments (**Fig. 7C,F**) were not different between wildtype and homozygous fr^{CR}/fr^{CR} animals. To summarize, untreated homozygous fr^{CR}/fr^{CR} animals showed no signs of altered colonic permeability, as evidenced by analysis of tight junction protein expression and TER, normal ENaC and Na^+,K^+-ATPase protein expression levels, but displayed reduced NHE1 and NHE3 protein expression levels.

DSS treatment rapidly induces severe diarrhea and inflammation in fr^{CR}/fr^{CR} rats

Induction of DSS-induced colitis equally lead to a slight but not significant body weight loss in all groups (**Fig 8A**). Already after 3 days of DSS treatment, homozygous mutant rats exhibited maximal diarrhea score and a significantly higher disease activity index that was maintained high throughout the (DSS) treatment (**Fig. 8B,C**). Control and heterozygous mutant animals developed increasingly severe diarrhea over the 7 days of treatment without ever reaching maximal diarrhea score (**Fig. 8B**); the disease activity index in fr^{CR}/+ animals was not significantly different from the wildtype group (**Fig. 8C**).

At the end of 7 days of DSS treatment, all groups showed an increase in the histology score that was significantly increased in the homozygous mutant rats as compared to the wildtype and heterozygous mutant rats (**Fig. 3B**). In all experimental groups, we observed a total decrease in the gland density, fibrosis of the submucosa and the lamina propria, and inflammatory infiltrates within gaps in the lamina muscularis mucosa (**Fig. 9**). In wildtype animals, the lamina muscularis mucosa appeared more frequently interrupted than in the other two groups, with mainly submucosal infiltrating macrophages, but overall an intact epithelium (**Fig. 9**). Heterozygous animals displayed muscular hypertrophy, shortened crypts, hyperplastic ganglia and an increased presence of lymphocytes (**Fig. 9**). In the homozygous mutant rats, a further striking decrease in the number of goblet cells (**Fig. 2A,B**) and rearrangements of the lamina propria (**Fig. 9**) were detected, and the overall inflammatory signs appeared more severe, with presence of neutrophils, eosinophils, and macrophages at the base of crypts, along with signs of cryptitis and edema of the lamina propria. Additionally, fr^{CR}/fr^{CR} animals presented ulcerations **(Fig. 9***)*. The mRNA transcript expression levels of *TNFα, TGFβ1, iNOS, IL-1β, IL-6, IL-12, IL-18, PAR2, matriptase, MMP3* and *CXCL-2* were all highly increased in homozygous fr^{CR}/fr^{CR} rats (**Fig. 4A-E,G-L**) as compared to both wildtype and heterozygous mutants, except for *IL-10*, where the mRNA transcript expression levels remained similar between the genotypes (**Fig. 4F**). Heterozygous $fr^{CR}/+$ animals showed similar mRNA transcript expression levels for all cytokines compared to wildtype animals (**Fig. 4A-L**).

fr^{CR}/fr^{CR} rats exhibit severe bloody diarrhea and a delay in recovery

At the end of the recovery phase, all groups regained weight; the gain was, surprisingly, significantly higher in fr^{CR}/fr^{CR} rats as compared to wildtypes (**Fig. 8A**). Although delayed, the disease activity index as well as the diarrhea score in the fr^{CR}/fr^{CR} group dropped down to

wildtype and heterozygous mutant values (**Fig. 8B,C**). Before, during, and after the treatment and recovery phase, the colon length gradually shortened in all groups, but was not significantly different between the genotypes **(Fig. 8D)**. Following the recovery phase, all genotypes showed an increase in the histology score as compared to the score obtained after 7 days of DSS treatment (**Fig. 3C**). Following recovery, we assessed the mRNA transcript expression levels of different inflammatory and remodeling markers in animals after 7 days of DSS treatment and 7 days of recovery. After 14 days of treatment, +/+, fr^{CR}/+ and fr^{CR}/fr^{CR} animals presented similar levels of mRNA transcript expression levels for *TNFα, TGFβ1*, *IL-1β IL-6, IL-10, IL-12, IL-18, PAR2, matriptase,* and *MMP3* (**Fig. 4A,B,D-K**), whereas *iNOS* expression was about twice as high and *CXCL2* expression 7-fold increased in the homozygous mutant rats as compared to the untreated fr^{CR}/fr^{CR} animals (**Fig. 4C,L**). Although not significantly different among the groups, the expression levels of *TNFα* appeared generally elevated in all genotypes as compared to untreated groups (**Fig. 4A**).

The protein expression levels of sodium transporters are not altered in fr^{CR}/fr^{CR} rats following DSS treatment

We further analyzed whether the severe diarrhea observed in homozygous mutants following DSS treatment and recovery phase could be correlated with a decreased ENaC or sodium transporter protein expression in the colon (**Figs. 10 and 11**). Surprisingly, at the protein expression level no differences could be detected between the groups neither for the sodium-hydrogen exchangers 1 and 3 (NHE1 and NHE3), and the Na^+, K^+-ATPase (**Fig. 10A-D**), nor for the full-length α-, β-, and γ-ENaC subunits (**Fig. 11A,B,D,E**), or the cleaved α- and γ-ENaC fragments (**Fig. 11C,F**). The I_{sc} and the TER were not significantly different between wildtype and homozygous fr^{CR}/fr^{CR} mutant rats (**Fig. 5H,I**), despite a reduction in the protein level for ZO-1, but not for occludin and claudin-1 in fr^{CR}/fr^{CR} rats (**Fig. 5E-G**).

fr^{CR}/fr^{CR} rats exhibit severe architectural remodeling with crypt branching

At the histological level, all genotypes displayed strongly decreased number of goblet cells (**Fig. 2A,B**), lesser crypts, absence of mucosecretory capacity of the epithelium, ulcerations, and architectural alterations with crypt branching; the latter was however less present in heterozygous animals (**Fig. 12**). Colons of wildtype animals still presented severe signs of acute inflammation, with increasing amounts of leucocytes and lymphocytes in the epithelium, edemas of the lamina propria, and presence of eosinophils, fibrine and pus in the lumen (**Fig. 12).** Heterozygous animals showed milder signs of inflammation and ulceration, in most cases already re-epitheliarized, than wildtype and homozygous mutant rats (**Fig. 12**). Homozygous mutants reached a significantly higher score than both wildtype and heterozygous animals on day 14 (**Fig. 3C**). Here, the higher score of fr^{CR}/fr^{CR} rats reflected the strong architectural remodeling with high presence of branched crypts (**Fig. 12**). fr^{CR}/fr^{CR} rats displayed severe signs of inflammation and presence of pus in the lumen; additional localized angiodysplasia was observed (**Fig. 12**).

In summary, prostasin seems to have a protective role against DSS-induced inflammation. Altered prostasin leads to increased and faster tissue remodeling following DSS treatment.

Discussion

frCR/frCR rats exhibit an intestinal/epithelial defect that affects the colonic integrity

In the present study, we tested whether prostasin-mutant fr^{CR}/fr^{CR} rats, that show all signs of an epithelial dysfunction, are more prone to develop an experimentally DSS-induced colitis. We previously unveiled a lower body weight, an increased transepidermal water loss, and diarrhea.[21] Body weight loss is often linked to dehydration defects caused by either skin or intestine anomalies as evidenced in human and rodents.[42-44] A more detailed analysis in colon

of these fr^{CR}/fr^{CR} rats additionally unveiled a reduced number of crypt and goblet cells (**Figs. 1 and 2**), that is indicative for a dysbalance of the intestinal homeostasis.[45] Moreover, local inflammation could be observed together with mild edema, however without signs of infiltrating leucocytes or macrophages. Interestingly, the histological analysis of colon-specific prostasin knockout mice shows no colonic alterations, and the mice are indistinguishable from the control group.[24] There is no apparent effect on the number of crypt cells, a normal intestine length-to–body weight ratio, no leaky intestinal permeability following fluorescein isothiocyanate dextran supply in blood plasma, and no signs of increased stool hydration or diarrhea, indicating an overall intact intestinal barrier function.[24] This might be a tissue-specific phenomenon, since epidermis-specific prostasin (CAP1/Prss8) knockout mice display a severely impaired epidermal barrier function that results in significantly increased transepithelial water loss. These mice die shortly after birth due to a rapid and fatal dehydration through the skin.[19] Complete absence of the tight junction protein occludin and leakiness of the tight junctions in the stratum granulosum are likely causative.[19] Alternatively, the G54-P57 deletion[26] may induce additional effects through the modified interaction of prostasin with its potential effectors/targets, since we previously reported a considerable impact on the protein folding of the fr^{CR}/fr^{CR} mutation.[21] Thereby, by comparing both prostasin mouse and rat mutants, a species- and tissue-specificity may account for our findings. *fr/fr* mice harboring a spontaneous V170D prostasin mutation that predicts a similar loss of protein stability as in fr^{CR}/fr^{CR} rats show no signs of colonic barrier dysfunction, like diarrhea or morphological alterations.[21] Interestingly, untreated fr^{CR}/fr^{CR} animals did not show altered expression of tight junction proteins in the colon (**Fig. 5A-D**). Moreover, colonic I_{sc} and transepidermal resistance were similar between wildtype and homozygous mutant animals without treatment (**Fig. 5H,I**). After recovery, despite reduced ZO-1 protein

expression (**Fig. 5E**), the I_{sc} and TER were not changed between controls and fr^{CR}/fr^{CR} rats, indicating that the fr^{CR} mutation does not affect the colonic permeability.

In normal human distal colon and rectum, electrogenic Na^+ absorption (mediated by the epithelial Na^+ channel, ENaC) is the dominant Na^+ absorptive process and accounts for the substantial lumen-negative transmucosal electrical potential difference (PD).[46] A loss of this PD is the hallmark of mucosal inflammation in active ulcerative colitis (UC), is proportional with impaired electrogenic Na^+ absorption, and reflects marked dysfunction of apically located ENaC.[14,47] Interestingly, ENaC-mediated electrogenic Na^+ absorption is also markedly impaired in the non-inflamed sigmoid colon of patients with active CD of the terminal ileum.[48] Thereby, down-regulation of ENaC with reduction in sodium reabsorption in colon was hypothetized to contribute to diarrhea associated with inflammatory bowel disease.[14,48] In colon-specific (α)ENaC knockout mice, the morphology of the adult distal colon including colon epithelium and mucin-secreting goblet cells macroscopically appears to be normal without any effect on the number of crypt cells or difference in the intestine length-to-body weight ratio, or signs of diarrhea.[24] As the amiloride-sensitive rectal potential difference is significantly reduced in fr^{CR}/fr^{CR} rats,[21] we asked the question whether reduced ENaC activity, due to altered prostasin protein expression, is a predisposing factor to develop more rapidly and/or more severely a DSS-induced colitis.

Prostasin protects against DSS-induced inflammation

Although no leucocyte and macrophage infiltrations could be observed in untreated fr^{CR}/fr^{CR} rats, *iNOS* mRNA transcript expression levels were significantly increased, both with and without DSS treatment (**Fig. 4C**). In this context it is worthwhile mentioning that induced iNOS expression has been described to protect against pathogen infections.[49] Equally, *TGFβ1, PAR2* and *MMP3* mRNA transcript expression levels were significantly reduced (**Fig.**

3B,J,L). This decrease might be linked, since TGFβ1 was previously shown to induce MMPs and PAR2 expression, and PAR2-mediated IL-6 secretion,[50,51] even though here no change could be detected at the mRNA transcript expression level of IL-6 in untreated homozygous mutants and after DSS treatment and recovery **(Fig. 4E)**. PAR-2 was previously identified as a downstream target of prostasin.[43] It is expressed in mouse distal colon, and seems to stimulate Cl^- and K^+ secretion while inhibiting the baseline Na^+ reabsorption.[52] Even though PAR2 was previously identified as non-crucial in the pathogenesis of experimental DSS-induced colitis, as tested in PAR2 knock-out mice,[6] the receptor was shown upregulated in mast cells from patients with ulcerative colitis and Crohn's disease.[53,54] The mRNA transcript expression levels of PAR2 where indeed highly increased after 7 days of DSS treatment in homozygous mutants, but not significantly different after recovery (**Fig. 4I**).

Following 7 days of DSS treatment, the wildtype, heterozygous and homozygous fr^{CR}/fr^{CR} animals showed signs of acute inflammation along with strong reductions in the number of goblet cells (**Fig. 2**), rearrangements of the lamina propria, and signs of fibrosis. However, the observed alterations were more severe in homozygotes, which also additionally presented edema and ulcerations (**Figs. 3 and 9**). This is consistent with the clinical parameters as described by Cooper and colleagues,[27] revealing highest diarrhea score with rectal bleeding, a common symptom of IBD[1], and highest disease activity index already at day 3 for fr^{CR}/fr^{CR} rats, while wildtype and heterozygotes never reached the maximal score (**Fig. 8**). This is also consistent with the mRNA transcript expression levels measured after 7 days of treatment. Colons of homozygous mutant animals displayed highly increased levels of all tested cytokines and remodeling markers as compared to both wildtype and heterozygous rats, except for *IL-10* that remained similar among the genotypes (**Fig. 4**). Absence of IL-10 up-regulation is in line with the increase of all other cytokines, since it exerts generally an immunoregulatory action on pro-inflammatory cytokines,[55] like e.g. TNFα. The strong

increase in pro-inflammatory TNFα mRNA transcript expression that we could measure in homozygous mutants (**Fig. 4A**) is also a known feature in IBD, and TNFα-inhibitors are the most common drugs used in the treatment for UC.[56] The increased mRNA transcript expression levels seen for IL-1β, IL-6, IL-12, IL-18 and TGFβ1 in homozygous mutant animals (**Fig. 4**) are also observed in patients. Elevated mRNA transcript expression levels of IL-1β and IL-18 were measured in intestinal specimen from IBD patients.[57-59] Currently, antibodies and agents targeting the pro-inflammatory IL-6 and IL-12 are studied in clinical trials.[60] The anti-inflammatory cytokine TGFβ1 was shown as strongly increased, but inactive due to blockade of its receptor by Smad7, leading to the development of Smad7-targeting agents for the treatment of IBD.[61]

It is quite likely that decreased ENaC activity due to reduced prostasin expression is responsible for the severe watery diarrhea in homozygous mutant rats after DSS treatment. Similarly, other ion transporters have been linked to UC predisposition and pathogenesis, such as e.g. the sodium hydrogen exchanger 3 (NHE3), whose deletion in mice leads to elevated mortality during DSS-induced colitis.[62] In patients suffering from IBD, several transporters including the Na^+, K^+-ATPase, NHE1, NHE3, β-ENaC, NHERF1,2, and CLC-5 appear downregulated at the protein level.[63] Similarly, down-regulation of sodium transporters and their associated regulatory proteins were observed in DSS- and TNBS- treated mice.[63] The authors stipulated that a coordinated down-regulation of multiple sodium transporters and their regulatory proteins might be responsible for IBD-associated diarrhea. In line with this observation, we could detect reduced protein expression for NHE1 and NHE3 in untreated homozygous fr^{CR}/fr^{CR} animals, while the levels for the Na^+,K^+-ATPase and α-, β-, and γ-ENaC remained unchanged between genotypes (**Figs. 6 and 7**), although after treatment none of the protein expression levels was significantly different between the genotypes **(Figs. 10 and 11).**

Other proteases or regulatory proteins likely involved in the same cascade might be implicated as well. Intestine-specific deletion of matriptase, a proposed upstream activator of prostasin,[64] results in lethality several weeks after weaning due to severe diarrhea and massive intestinal inflammation, resulting in complete breakdown of the mucosal barrier function and overall colonic architecture.[65] During DSS-induced injury, matriptase is downregulated in wildtype mice as well as in colonic epithelium from IBD patients, and thus hypomorphic St14 mice with low matriptase expression are severely delayed in recovering from DSS-induced colitis.[6] Interestingly, also increased prostasin and/or matriptase expression may be causative for histological abnormalities, since the intestine-specific deletion of hepatocyte growth factor activator inhibitor 1 (HAI-1, also known as serine protease inhibitor Kunitz type 1 or SPINT1), an inhibitor of matriptase[66] and prostasin as shown in vitro (Hummler *et al.*, unpublished data), affects the intestinal integrity, worsening the colonic phenotype following DSS treatment.[67] Interestingly, mutations in HAI-2 (or SPINT2) have been linked to a syndromic form of congenital sodium diarrhea in human patients,[68,69] where prostasin-induced ENaC-mediated sodium currents are no longer inhibited.[70] In this study, unlike in human samples,[6] matriptase was highly increased at the mRNA transcript expression level in homozygous mutants after 7 days of treatment, but similarly expressed as in control animals without treatment and after recovery (**Fig. 4J**). This result suggests a more complex protease network, where upregulation of matriptase might be a compensation for mutated prostasin in rats. In summary, intact colonic sodium transport is required for intestinal integrity and transport alterations cause diarrhea that is one of the common symptoms of IBD. Lack of prostasin thus predisposes to the development of DSS-induced colitis, without however altering ENaC protein expression. Interestingly, after treatment and recovery, the amiloride-sensitive I_{sc} was completely abolished in both wildtype and homozygous fr^{CR}/fr^{CR} colons (data not shown). The same was observed in *ex vivo* epithelial preparations from UC patients,

where the response to amiloride was nearly completely absent, likely due to cytokine-induced downregulation of β- and γ-ENaC.[14] In our study, however, the protein expression levels of α-, β-, and γ-ENaC were not different between the genotypes, both in untreated and in DSS-treated animals (**Figs. 7 and 11**). In consensus with our data, cytokines can impact ENaC activity: TNFα is able to directly activate ENaC by binding to the C-terminal domain of α-ENaC during pulmonary inflammation,[71] whereas upregulation of TGFβ1 drives internalization of ENaC during acute respiratory distress syndrome,[72] likely via increased reactive oxygen species production.[72,73]

Prostasin is required for the architectural integrity of the colon and protects from remodeling

During the recovery phase, the diarrhea score and disease activity index gradually decreased in all genotypes over the 7 days of recovery with water (**Fig 8**), but were significantly delayed in the homozygous mutant fr^{CR}/fr^{CR} rats. Surprisingly, the body weight was even significantly higher in fr^{CR}/fr^{CR} rats as compared to wild-type at the end of the recovery phase (**Fig. 8A**). These observations are surprising since despite severe bloody diarrhea during 6 days (**Fig. 8B**), and highly increased cytokine mRNA transcript expression levels during the treatment (**Fig. 4**), and although delayed, homozygous mutants achieved to recover to a similar level as wildtype and heterozygous $fr^{CR}/+$ animals. This might be a consequence of the basal inflammatory profile of the homozygous mutants, enabling them to recover in a more efficient way than wildtype and heterozygous rats. We could moreover measure increased mRNA transcript expression levels for the remodeling markers MMP3 and CXCL2[74] during the treatment in fr^{CR}/fr^{CR} animals (**Fig. 4K,L**), which might also contribute to the enhanced recovery. We previously reported in the skin of these rats mislocalisation of hair follicles.[21] Since this is an innate feature, there are no signs of acute inflammation in the epidermis of fr^{CR}/fr^{CR} mutant animals. In a similar way, we hypothesize that the inflammatory profile in the

colon of untreated homozygous mutants might be innate, potentially leading to habituation of the epithelium to local inflammations. Similarly, TGFβ1-dependent down-regulation of T cell responses in patients was proposed to attenuate the response to harmless constituents of the endogenous microflora.[75] Accordingly, the histopathological analysis revealed that fr^{CR}/fr^{CR} rats showed predominantly signs of chronic inflammation, together with important architectural modifications of the mucosa and the colonic epithelium; occasionally, we observed angiodysplasia (**Figs. 1, 3 and 12**). Wildtype and heterozygous mutants still displayed signs of rather acute inflammation, even though the observed features were milder in heterozygous rats compared to controls (**Figs. 12 and 3**). The evolution towards chronicity is thus more rapid in homozygous mutants than in wildtype and heterozygous animals. In line with this observation, we could measure in homozygous mutants highly increased mRNA transcript expression levels of CXCL2 (**Fig. 4L**), a proposed dysplastic and remodeling marker,[76] that was strongly associated with dysplasia-carcinoma transition in human samples.[77] Despite the fact that control and heterozygous rats displayed signs of acute inflammation, the mRNA levels for inflammatory markers were not different between the genotypes after recovery, except for *iNOS* that was significantly increased in fr^{CR}/fr^{CR} animals (**Fig. 5**).

Taken together, these observations reveal a complex protease network where prostasin is implicated in the regulation of intestinal inflammation and susceptibility towards acute colitis. According to our results, prostasin is also implicated in this regulating network, and might be implicated in the protection against inflammation. Mutation of prostasin leads to reduced ENaC activity, NHE1 and NHE3 protein expression, and might increase inflammatory response. Therapies enhancing the protective activity of prostasin need further investigations in IBD patients.

Acknowledgements

We want to thank Prof. Bernard C. Rossier for his helpful suggestions, and all the members of the Hummler laboratory for useful discussions. We are grateful to the Mouse Pathology Facility and Jean-Christophe Stehle for paraffin embedding and preparation of H&E sections.

References

1. de Mattos B, Garcia M, Nogueira J, et al. Inflammatory bowel disease: an overview of immune mechanisms and biological treatments. *Mediators Inflamm*. 2015;2015:493012.
2. Antalis T, Shea-Donohue T, Vogel S, et al. Mechanisms of disease: protease functions in intestinal mucosal pathobiology. *Nat Clin Pract Gastroenterol Hepatol*. 2007;4:393-402.
3. Okayasu I, Hatakeyama S, Yamada M, et al. A novel method in the induction of reliable experimental acute and chronic ulcerative colitis in mice. *Gastroenterology*. 1990;98:694-702.
4. Melgar S, Karlsson A, Michaelsson E: Acute coliditis induced by dextran sulfate sodium progresses to chronicity in C57BL/6 but not in BALB/c mice: correlation between symptoms and inflammation. *Am J Physiol Gastrointest Liver Physiol*. 2005;288:1328-1338.
5. Melgar S, Karlsson A, Rehnstrom E, et al. Validation of murine dextran sulfate sodium-induced colitis using four therapeutic agents for human inflammatory bowel disease. *Int Immunopharmacol*. 2008;8:836-844.
6. Netzel-Arnett S, Buzza M, Shea-Donohue T, et al. Matriptase protects against experimental colitis and promotes intestinal barrier recovery. *Inflamm Bowel Dis*. 2012;18:1303-1314.
7. Poritz L, Garver K, Green C, et al. Loss of tight junction protein ZO-1 in dextran sulfate sodium induced colitis. *J Surg Res*. 2007;140:12-19.
8. Murphy M, Eastham E, Nelson R, et al. Intestinal permeability in Crohn's disease. *Arch Dis Child*. 1989;64:321-325.
9. Tibble J, Sigthorsson G, Bridger S, et al. Surrogate markers of intestinal inflammation

529 are predicitive of relapse in patients with inflammatory bowel disease.
530 *Gastroenterology*. 2000;119:15-22.
531 **10.** Wyatt J, Vogelsang H, Hubl W, et al. Intestinal permeability and the prediction of
532 relapse in Crohn's disease. *Lancet*. 1993;341:1437-1439.
533 **11.** Barmeyer C, Schulzke J, Fromm M: Claudin-related intestinal diseases. *Semin Cell*
534 *Dev Biol*. 2015;42:30-38.
535 **12.** Gomez-Gomez G, Masedo A, Yela C, et al. Current stage in inflammatory bowel
536 disease: what is next? *World J Gastroenterol*. 2015;21:11282-303.
537 **13.** Knights D, Lassen K, Xavier R: Advances in inflammatory bowel disease
538 pathogenesis: linking host genetics and the microbiome. *Gut*. 2013;62:1505-1510.
539 **14.** Amasheh S, Barmeyer C, Koch C, et al. Cytokine-dependent transcriptional down-
540 regulation of epithelial sodium channel in ulcerative colitis. *Gastroenterology*.
541 2004;126:1711-1720.
542 **15.** Barmeyer C, Amasheh S, Tavalali S, et al. IL-1beta and TNFalpha regulate sodium
543 absorption in rat distal colon. *Biochem Biophys Res Commun*. 2004;317:500-507.
544 **16.** Vuagniaux G, Vallet V, Jaeger N, et al. Activation of the amiloride-sensitive epithelial
545 sodium channel by the serine protease mCAP1 expressed in a mouse cortical
546 collecting duct cell line. *J Am Soc Nephrol*. 2000;11:828-834.
547 **17.** Vuagniaux G, Vallet V, Jaeger N, et al. Synergistic activation of ENaC by three
548 membrane-bound channel-activating serine proteases (mCAP1, mCAP2, and mCAP3)
549 and serum- and glucocorticoid-regulated kinase (Sgk1) in Xenopus oocytes. *J Gen*
550 *Physiol*. 2002;120:191-201.
551 **18.** Vallet V, Pfister C, Loffing J, et al. Cell-surface activation of near-silent epithelial
552 Na+ channels. *J Am Soc Nephrol*. 2002;13:588-594.

553 **19.** Leyvraz C, Charles R, Rubera I, et al. The epidermal barrier function is dependent on
554 the serine protease CAP1/Prss8. *The Journal of Cell Biology*. 2005;170:487-496.
555 **20.** Hummler E, Dousse A, Rieder A, et al. The channel-activating protease CAP1/Prss8
556 is required for placental labyrinth maturation. *PLoS One*. 2013;8:e55796.
557 **21.** Frateschi S, Keppner A, Malsure S, et al. Mutations of the serine protease CAP1/Prss8
558 lead to reduced embryonic viability, skin defects, and decreased ENaC activity. *Am J*
559 *Pathol*. 2012;181:605-615.
560 **22.** Verouti S, Boscardin E, Hummler E, et al. Regulation of blood pressure and renal
561 function by NCC and ENaC: lessons from genetically engineered mice. *Curr Opin*
562 *Pharmacol*. 2015;21:60-72.
563 **23.** Planès C, Randrianarison N, Charles R, et al. ENaC-mediated alveolar fluid clearance
564 and lung fluid balance depend on the channel-activating protease 1. *EMBO Mol Med*.
565 2010; 2:26-37.
566 **24.** Malsure S, Wang Q, Charles R, et al. Colon-specific deletion of epithelial sodium
567 channel causes sodium loss and aldosterone resistance. *J Am Soc Nephrol*. 2014;
568 25:1453-1464.
569 **25.** Panteleyev A, Christiano A: The Charles River "Hairless" rat mutation is distinct from
570 the Hairless mouse allele. *Comp Med*. 2001;51:49-55.
571 **26.** Spacek D, Perez A, Ferranti K, et al. The mouse frizzy (fr) and rat "hairless" (frCR)
572 mutations are natural variants of protease serine S1 family member 8 (Prss8). *Exp*
573 *Dermatol*. 2010;19:527-532.
574 **27.** Cooper H, Murthy S, Shah R, et al. Clinicopathologic study of dextran sulfate sodium
575 experimental murine colitis. *Lab Invest*. 1993;69:238-249.

576 **28.** Rath H, Herfarth H, Ikeda J, et al. Normal luminal bacteria, especially Bacteroides
577 species, mediate chronic colitis, gastritis, and arthritis in HLA-B27/human beta2
578 microglobulin transgenic rats. *J Clin Invest*. 1996;98:945-953.
579 **29.** Khan H, Abdelhalim M, Alhomida A, et al. Transient increase in IL-1b, IL-6 and
580 TNF-a gene expression in rat liver exposed to gold nanoparticles. *Genet Mol Res*.
581 2013;12:5851-5857.
582 **30.** Shynlova O, Tsui P, Dorogin A, et al. The expression of transforming growth factor
583 beta in pregnant rat myometrium is hormone and stretch dependent. *Reproduction*.
584 2007;134:503-511.
585 **31.** Chen C, Chen Q, Ouyang Q, et al. Transient early neurotrophin release and delayed
586 inflammatory cytokine release by microglia response to PAR-2 stimulation. *J*
587 *Neuroinflammation*. 2012;9:142.
588 **32.** Moreira T, Cebere A, Cebers G, et al. Reduced HO-1 protein expression is associated
589 with more severe neurodegeneration after transient ischemia induced by cortical
590 compression in diabetic Goto-Kakizaki rats. *J Cereb Blood Flow Metab*.
591 2007;27:1710-1723.
592 **33.** Houdeau E, Moriez R, Leveque M, et al. Sex steroid regulation of macrophage
593 migration inhibitory factor in normal and inflamed colon in the female rat.
594 *Gastroenterology*. 2007, 132:982-93.
595 **34.** Camuesco D, Comalada M, Rodriguez-Cabezas E, et al. The intestinal anti-
596 inflammatory effect of quercitrin is associated with an inhibition in iNOS expression.
597 *Br J Pharmacol*. 2004,143:908-18.
598 **35.** Rubera I, Loffing J, Palmer L, et al. Collecting duct-specific gene inactivation of
599 alphaENaC in the mouse kidney does not impair sodium and potassium balance. *J*
600 *Clin Invest*. 2003;112:554-565.

36. Girardet M, Geering K, Frantes J, et al. Immunochemical evidences for a transmembrane orientation of both the (Na+,K+)-ATPase subunits. *Biochem J*. 1981;20:6684-6691.

37. Perrier R, Boscardin E, Malsure S, et al. Severe salt-losing syndrome and hyperkalemia in adult kidney specific aENaC knockouts. *J Am Soc Nephrol*. 2015;2015020154

38. Hummler E, Mérillat A, Rubera I, et al. Conditional gene targeting of the Scnn1a (alphaENaC) gene locus. *Genesis*. 2002;32:169-172.

39. Traykova-Brauch M, Schönig K, Greiner O, et al. An efficient and versatile system for acute and chronic modulation of renal tubular function in transgenic mice. *Nat Med*. 2009;14:979-984.

40. Mérillat A, Charles R, Porret A, et al. Conditional gene targeting of the ENaC subunit genes Scnn1b and Scnn1g. *Am J Physiol Renal Physiol*. 2009;296:249-256.

41. Bertog M, Cuffe J, Pradervand S, et al. Aldosterone responsiveness of the epithelial sodium channel (ENaC) in colon is increased in a mouse model for Liddle's syndrome. *J Physiol*. 2008,586:459-75.

42. Koletzko S, Osterrieder S: Acute infectious diarrhea in children. *Dtsch Artzebl Int*. 2009;106:539-547.

43. Frateschi S, Camerer E, Crisante G, et al. PAR2 absence completely rescues inflammation and ichthyosis caused by altered CAP1/Prss8 expression in mouse skin. *Nat Comm*. 2011;2:1-11.

44. Crisante G, Battista L, Iwaszkiewicz J, et al. The CAP1/Prss8 catalytic triad is not involved in PAR2 activation and protease nexin-1 (PN-1) inhibition. *FASEB J*. 2014;28:4792-4805.

625 **45.** Goll R, van Beelen Granlund A: Intestinal barrier homeostasis in inflammatory bowel
626 disease. *Scand J Gastroenterol*. 2015;50:3-12.
627 **46.** Sandle G: Infective and inflammatory diarrhoea: mechanisms and opportunities for
628 novel therapies. *Curr Opin Pharmacol*. 2011;11:634-639.
629 **47.** Greig E, Boot-Handford R, Mani V, et al. Decreased expression of apical Na+
630 channels and basolateral Na+, K+-ATPase in ulcerative colitis. *J Pathol*. 2004;204:84-
631 92.
632 **48.** Zeissig S, Bergann T, Fromm A, et al. Altered ENaC expression leads to impaired
633 sodium absorption in the noninflammed intestine in Crohn's disease. *Gastroenterology*.
634 2008;134:1436-1447.
635 **49.** Chakravortty D, Hensel M: Inducible nitric oxide synthase and control of intracellular
636 bacterial pathogens. *Microbes Infect*. 2003;5:621-627.
637 **50.** Yan C, Boyd D. Regulation of matric metalloproteinase gene expression. *J Cell*
638 *Physiol*. 2007,211:19-26.
639 **51.** Saito A, Osuga Y, Yoshino O, et al. TGF-b1 induces proteinase-activated receptor 2
640 (PAR2) expression in endometriotic stromal cells and stimulates PAR2 activation-
641 induced secretion of IL-6. *Hum Reprod*. 2011;26:1892-1898.
642 **52.** Cuffe J, Bertog M, Velasquez-Rocha S, et al. Basolateral PAR-2 receptors mediate
643 KCl secretion and inhibition of Na+ absorption in the mouse distal colon. *J Physiol*.
644 2002;539:209-222.
645 **53.** Kim J, Choi S, Yun K, et al. Expression of protease-activated receptor 2 in ulcerative
646 colitis. *Inflamm Bowel Dis*. 2003;9:224-229.
647 **54.** Christerson U, Keita A, Söderholm J, et al. Increased expression of protease-activated
648 receptor-2 in mucosal mast cells in Crohn's ileitis. *J Crohns colitis*. 2009;3:100-108.

649 **55.** Fonseca-Camarillo G, Yamamoto-Furusho J. Immunoregulatory pathways involved in
650 inflammatory bowel disease. *Inflamm Bowel Dis*. 2015,21:2188-93.
651 **56.** Park S, Jeen Y. Current and emerging biologics for ulcerative colitis. *Gut Liver*.
652 2015,9:18-27.
653 **57.** Casini-Raggi V, Kam L, Chong Y, et al. Mucosal imbalance of IL-1 and IL-1 receptor
654 antagonist in inflammatory bowel disease. A novel mechanism of chronic intestinal
655 inflammation. *J Immunol*. 1995,154:2434-40.
656 **58.** Monteleone G, Trapasso F, Parrello T, et al. Bioactive IL-18 expression is up-
657 regulated in Crohn's disease. *J Immunol*. 1999,163:143-7.
658 **59.** Pizarro T, Michie M, Bentz M, et al. IL-18, a novel immunoregulatory cytokine, is up-
659 regulated in Crohn's disease: expression and localization in intestinal mucosal cells. *J*
660 *Immunol*. 1999,162:6829-35.
661 **60.** Sands B. New drugs on the horizon for IBD. *Dig Dis*. 2014,32:74-81.
662 **61.** Marafini I, Zorzi F, Codazza S, et al. TGF-beta signaling manipulation as potential
663 therapy for IBD. *Curr Drug Targets*. 2013,14:1400-4.
664 **62.** Kiela P, Laubitz D, Larmonier C, et al. Changes in mucosal homeostasis predispose
665 NHE3 knockout mice to increased susceptibility to DSS-induced epithelial injury.
666 *Gastroenterology*. 2009;137:965-975.
667 **63.** Sullivan S, Alex P, Dassopoulos T, et al. Downregulation of sodium transporters and
668 NHERF proteins in IBD patients and mouse colitis models: potential contributors to
669 IBD-associated diarrhea. *Inflamm Bowel Dis*. 2009;15:261-274.
670 **64.** Netzel-Arnett S, Currie B, Szabo R, et al. Evidence for a matriptase-prostasin
671 proteolytic cascade regulating terminal epidermal differentiation. *J Biol Chem*.
672 2006;281:32941-32945.

673 **65.** List K, Kosa P, Szabo R, et al. Epithelial integrity is maintained by a matriptase-
674 dependent proteolytic pathway. *Am J Pathol*. 2009;175:1453-1463.
675 **66.** Lin C, Anders J, Johnson M, et al. Purification and characterization of a complex
676 containing matriptase and a Kunitz-type serine protease inhibitor from human milk. *J*
677 *Biol Chem*, 1999;274:18237-18242.
678 **67.** Kawaguchi M, Takeda N, Hoshiko S, et al. Membrane-bound serine protease inhibitor
679 HAI-1 is required for maintenance of intestinal epithelial integrity. *Am J Pathol*.
680 2011;179:1815-1826.
681 **68.** Heinz-Erian P, Müller T, Krabichler B, et al. Mutations in SPINT2 cause a syndromic
682 form of congenital sodium diarrhea. *Am J Hum Genet*. 2009;84:188-196.
683 **69.** Salomon J, Goulet O, Canioni D, et al. Genetic characterization of congenital tufting
684 enteropathy: epcam associated phenotype and involvement of SPINT2 in the
685 syndromic form. *Hum Genet*. 2014;133:299-310.
686 **70.** Faller N, Gautschi I, Schild L: Functional analysis of a missense mutation in the serine
687 protease inhibitor SPINT2 associated with congenital sodium diarrhea. *PLoS One*.
688 2014;9:e94267.
689 **71.** Czikora I, Alli A, Bao H, et al. A novel tumor necrosis factor-mediated mechanism of
690 direct epithelial sodium channel activation. *Am J Respir Crit Care Med*.
691 2014,190:522-32.
692 **72.** Peters D, Vadasz I, Wujak L, et al. TGF-_beta directs trafficking of the epithelial
693 sodium channel ENaC which has implications for ion and fluid transport in acute lung
694 injury. *Proc Natl Acad Sci USA*. 2014,111:374-83.
695 **73.** Matalon S, Hardiman K, Jain L, et al. Regulation of ion channel structure and function
696 by reactive oxygen-nitrogen species. *Am J Physiol*. 2003,285:1184-9.

697 **74.** Sipos F, Germann T, Wichmann B, et al. MMP3 and CXCL1 are potent stromal
698 protein markers of dysplasia-carcinoma transition in sporadic colorectal cancer. *Eur J*
699 *Cancer Prev*. 2014, 23:336-43.
700 **75.** Del Zotto B, Mumolo G, Pronio A, et al. TGF-b1 production in inflammatory bowel
701 disease: differing production patterns in Crohn's disease and ulcerative colitis. *Clin*
702 *Exp Immunol*. 2003,134:120-6.
703 **76.** Tang A, Li N, Li X, et al. Dynamic activation of the key pathways linking colitis to
704 colorectal cancer in a mouse model. *Carcinogenesis*. 2012,33:1375-83.
705 **77.** Galamb O, Wichmann B, Sipos F, et al. Dysplasia-carcinoma transition specific
706 transcripts in colonic biopsy samples. *PLoS One*. 2012,7:1-10.

Criterion	Score					Add
	0	1	2	3	4	+0.5-+1 for each
Inflammatory cells	-	↑	↑↑	↑↑↑	↑↑↑	ulcer
Goblet cells	-	↓	↓↓	↓↓↓	↓↓↓	
Mucosa thickening	-	↑	↑↑	↑↑↑	↑↑↑	
Submucosa cell infiltration	-	-	↑	↑↑	↑↑↑	
Destruction of architecture	-	-	-	↑	↑↑	

Table 1. Histological score to quantify the degree of intestinal inflammation according to Rath and colleagues.[28] ↑, increased ; ↓, decreased. 0.5 points were added to re-epitheliarized ulcers, and 1 point was added for acute ulcers.

713 **Figure legends**

714

715 **Figure 1.** Representative H&E stained colon sections from untreated +/+, fr^{CR}/+, and fr^{CR}/fr^{CR}
716 animals (n=4 per genotype). Magnification 10x scale bar = 50μm, and 20x scale bar = 25μm.
717 The white box indicates the magnified zone of (angiodysplastic) blood vessels. Note the
718 presence of shorter crypt cells and angiodysplasia in fr^{CR}/fr^{CR} rats (*).

719

720 **Figure 2.** Representative Alcian blue stained colon sections from (**A**) untreated +/+, fr^{CR}/+,
721 and fr^{CR}/fr^{CR} animals (untreated, upper panel), following 7 consecutive days of DSS treatment
722 (7 days, middle panel) and following 7 days of DSS treatment and 7 days of recovery (14
723 days, lower panel). Magnification 10x scale bar = 50μm. (**B**) Quantification of goblet cells
724 from corresponding Alcian blue (AB)-stained colon sections from untreated (n=4 per
725 genotype), following 7 days of DSS treatment (7 days, n=3 per genotype), and following 7
726 days of DSS treatment and 7 days of recovery (14 days, n=5 per genotype). ** $p< 0.01$, ***
727 $p< 0.001$.

728

729 **Figure 3.** Histology score as determined (Rath *et al*. 1996) for (**A**), untreated +/+, fr^{CR}/+, and
730 fr^{CR}/fr^{CR} animals (n=4 per genotype), (**B**), following 7 days of DSS treatment (7 days, n=3 per
731 genotype), and (**C**), following 7 consecutive days of DSS treatment and 7 days of recovery
732 (14 days, n=5 per genotype). ** $p< 0.01$, *** $p< 0.001$.

733

734 **Figure 4.** Relative mRNA transcript expression levels of (**A**) *TNFα*, (**B**) *TGFβ1*, (**C**) *iNOS*,
735 (**D**) *IL-1β,* (**E**) *IL-6*, (**F**) *IL-10*, (**G**) *IL-12*, (**H**) *IL-18*, (**I**) *PAR2*, (**J**) *matriptase*, (**K**) *MMP3*,
736 and (**L**) *CXCL2* in colons from +/+, fr^{CR}/+, and fr^{CR}/fr^{CR} animals (untreated, n=4 per genotype),
737 after 7 days of DSS treatment (7 days, n=3 per genotype) or following 7 consecutive days of

738 DSS treatment and 7 days of recovery (14 days, n=5 per genotype). * p< 0.05, ** p< 0.01,
739 *** p< 0.001.
740
741 **Figure 5.** (**A**) Representative immunoblots of colon lysates from untreated (left panel) and
742 treated (7 days DSS and 7 days recovery, 14 days, right panel) +/+ and fr^{CR}/fr^{CR} rats with zona
743 occludens (ZO-1), occludin, claudin-1 and actin. Protein quantification of corresponding
744 immunoblots for untreated (**B-D**) and treated (14 days, **E-G**) animals for (**B, E**) zona-
745 occludens 1 (ZO-1), (**C, F**) occludin, and (**D, G**) claudin-1; n=6 for each genotype. Actin was
746 used as loading control. (**H**) Short circuit current (I_{sc}) and (**I**) transepidermal resistance (TER)
747 in proximal and distal colon of +/+ and fr^{CR}/fr^{CR} animals (untreated, n=3 per genotype) or
748 following 7 days of DSS treatment and 7 days of recovery (14 days, n=3 per genotype). (**J**)
749 Diarrhea score in untreated +/+, fr^{CR}/+, and fr^{CR}/fr^{CR} animals (n=4 per genotype). * p< 0.05.
750
751 **Figure 6.** (**A**), Representative immunoblots from colon lysates from untreated +/+, and
752 fr^{CR}/fr^{CR} rats for NHE1, NHE3 and Na^+, K^+-ATPase; actin was used as loading control (n=6
753 per genotype). (**B-D**) Corresponding protein quantification for (**B**), NHE1, (**C**), NHE3, and
754 (**D**), Na^+, K^+-ATPase. * p< 0.05.
755
756 **Figure 7.** (**A**), Representative immunoblots from colon lysates from untreated +/+, and
757 fr^{CR}/fr^{CR} rats for α-ENaC, β-ENaC and γ-ENaC; actin was used as loading control (n=6 per
758 genotype) (**B-F**) Corresponding protein quantification for (**B**), full-length (FL) and (**C**),
759 cleaved (Cl) α-ENaC, (**D**), full-length β-ENaC, (**E**), full-length (FL) and (**F**), cleaved (Cl) γ-
760 ENaC subunits (n=6 per genotype). Protein extracts from inducible kidney-specific Scnn1a,
761 Scnn1b and Scnn1g knock-out mice were used as negative controls for each immunoblot (Ctrl
762 KO). Actin was used as loading control.

763

764 **Figure 8**. Determination of clinical disease parameters during the course of the experiment (7
765 days of DSS treatment and 7 days of recovery) with (**A**), Δ body weight as % of initial BW
766 (g) from +/+ (n=8), fr^{CR}/+ (n=5), and fr^{CR}/fr^{CR} (n=8) rats. (**B**), diarrhea score from +/+ (n=8),
767 fr^{CR}/+ (n=5), and fr^{CR}/fr^{CR} (n=8) animals. (**C**), disease activity index from +/+ (n=8), fr^{CR}/+
768 (n=5), and fr^{CR}/fr^{CR} (n=8) animals. (**D**), mean colon length of +/+, fr^{CR}/+, and fr^{CR}/fr^{CR} animals
769 (untreated, n=4 per genotype), after 7 days of DSS treatment (7 days, n=3 per genotype), or
770 following 7 days of DSS treatment and 7 days of recovery (14 days, n=5 per genotype). *
771 $p<0.05$, ** $p<0.01$, *** $p<0.001$.

772

773 **Figure 9.** Representative H&E stained colon sections from +/+, fr^{CR}/+, and fr^{CR}/fr^{CR} animals
774 following 7 days of DSS treatment (n=3 per genotype). Magnification 10x scale bar = 50μm,
775 and 40x scale bar = 10μm. The white box indicates the magnified zone of inflammatory foci.
776 † : inflammatory infiltrations, ‡ : hypertrophy, ¶ : fibrosis, Δ : edema, # : acute ulcer, M :
777 macrophage, E : eosinophil, N : neutrophil.

778

779 **Figure 10.** (**A**), Representative immunoblots and corresponding protein quantification of (**B**),
780 NHE1, (**C**), NHE3, and (**D**), Na^+, K^+-ATPase in colons from +/+, fr^{CR}/+, and fr^{CR}/fr^{CR} (n=5
781 per genotype) rats following 7 days of DSS treatment and 7 days of recovery. Actin was used
782 as loading control.

783

784 **Figure 11.** (**A**), Representative immunoblots and corresponding protein quantification of (**B**),
785 full-length (FL) and (**C**), cleaved (Cl) α-ENaC, (**D**), full-length β-ENaC, (**E**), full-length (FL)
786 and (**F**), cleaved (Cl) γ-ENaC subunits in colons from +/+, fr^{CR}/+, and fr^{CR}/fr^{CR} (n=5 per
787 genotype) rats following 7 days of DSS treatment and 7 days recovery. Protein extracts from

788 inducible kidney-specific Scnn1a, Scnn1b and Scnn1g knock-out mice were used as negative
789 controls for each immunoblot (Ctrl KO). Actin was used as loading control.
790
791 **Figure 12**. Representative H&E stained colon sections from +/+, fr^{CR}/+, and fr^{CR}/fr^{CR} animals
792 following 7 days of treatment plus 7 days of recovery (n=5 per genotype). Magnification 10x
793 scale bar = 50μm, and 40x scale bar = 10μm. The white box indicates the magnified zone of
794 inflammatory foci. † : inflammatory infiltrations, Δ : edema, ∞ : crypt branching, # : acute
795 ulcer, § : re-epitheliarized ulcer, * : angiodysplasia, M : macrophage, E : eosinophil.
796
797
798
799

Criterion	Score					Add
	0	1	2	3	4	+0.5-+1 for each
Inflammatory cells	-	↑	↑↑	↑↑↑	↑↑↑	ulcer
Goblet cells	-	↓	↓↓	↓↓↓	↓↓↓	
Mucosa thickening	-	↑	↑↑	↑↑↑	↑↑↑	
Submucosa cell infiltration	-	-	↑	↑↑	↑↑↑	
Destruction of architecture	-	-	-	↑	↑↑	

Table 1. Histological score to quantify the degree of intestinal inflammation according to Rath and colleagues.[28] ↑, increased ; ↓, decreased. 0.5 points were added to re-epitheliarized ulcers, and 1 point was added for acute ulcers.

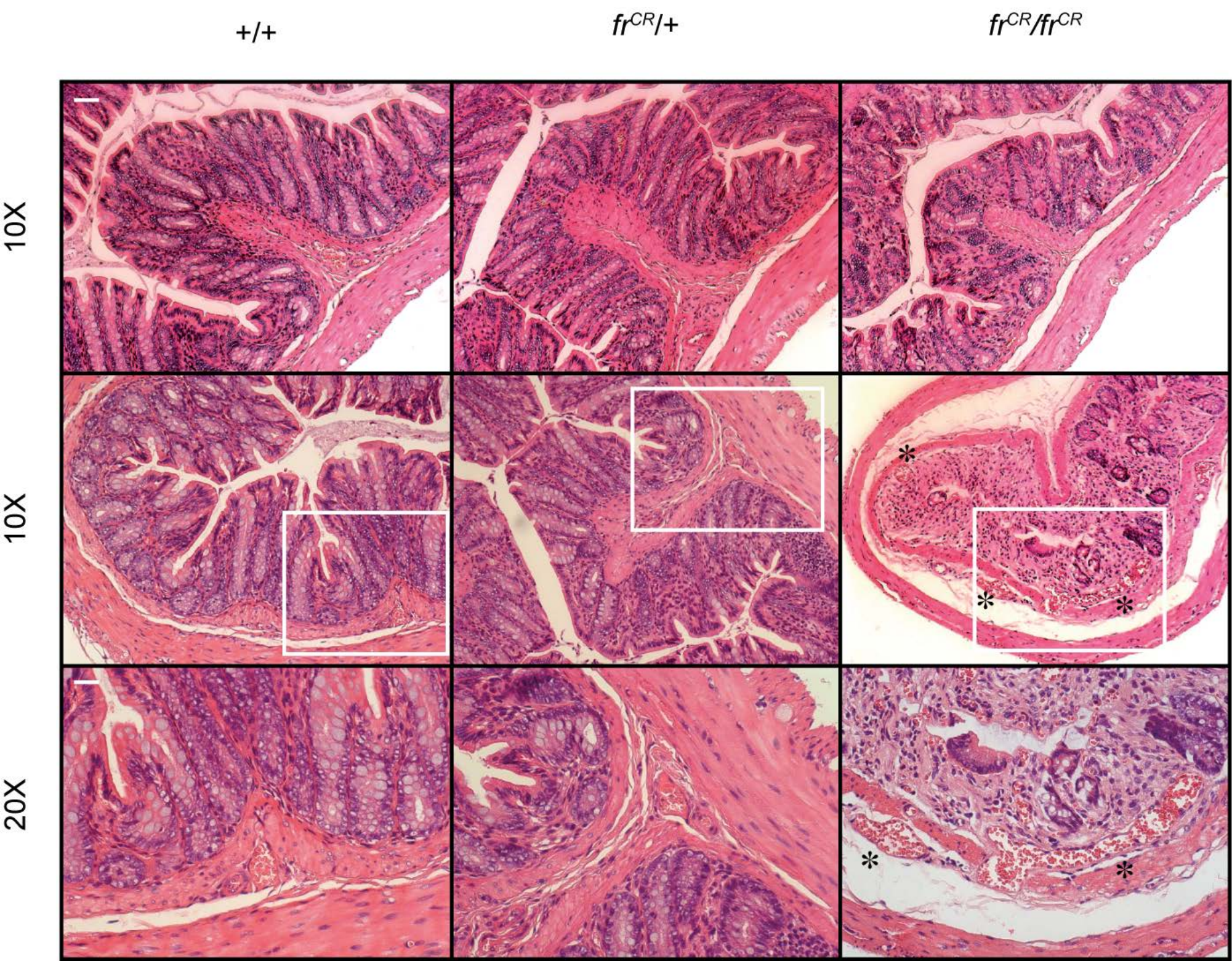
+/+
fr^{CR}/+
fr^{CR}/fr^{CR}
10X
10X
20X

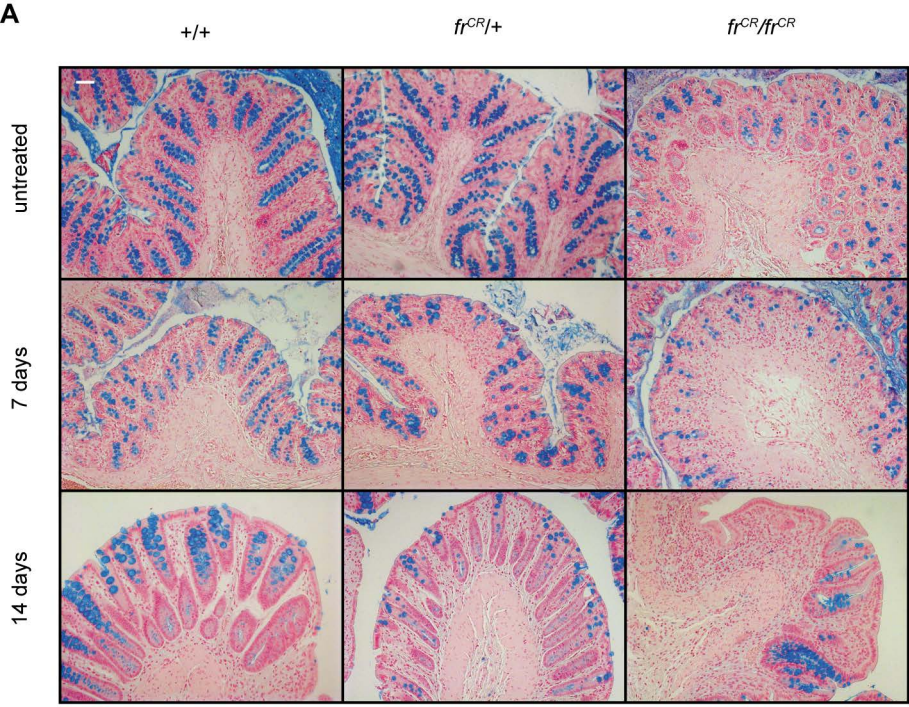
A
+/+
fr^CR/+
fr^CR/fr^CR
untreated
7 days
14 days

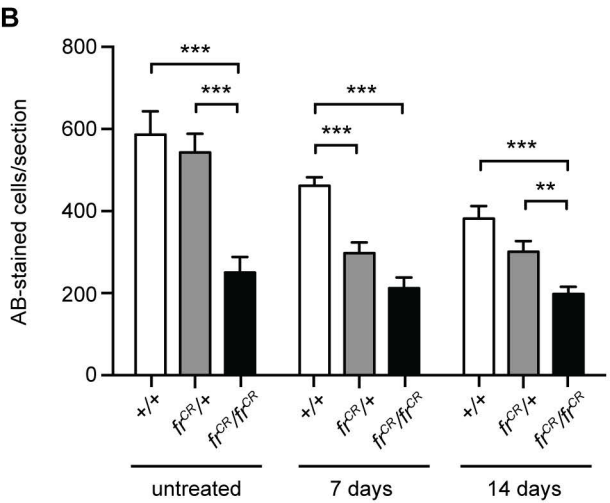
B
AB-stained cells/section
800
600
400
200
0
***
***
***
***
***
**
+/+
fr^CR/+
fr^CR/fr^CR
untreated
7 days
14 days

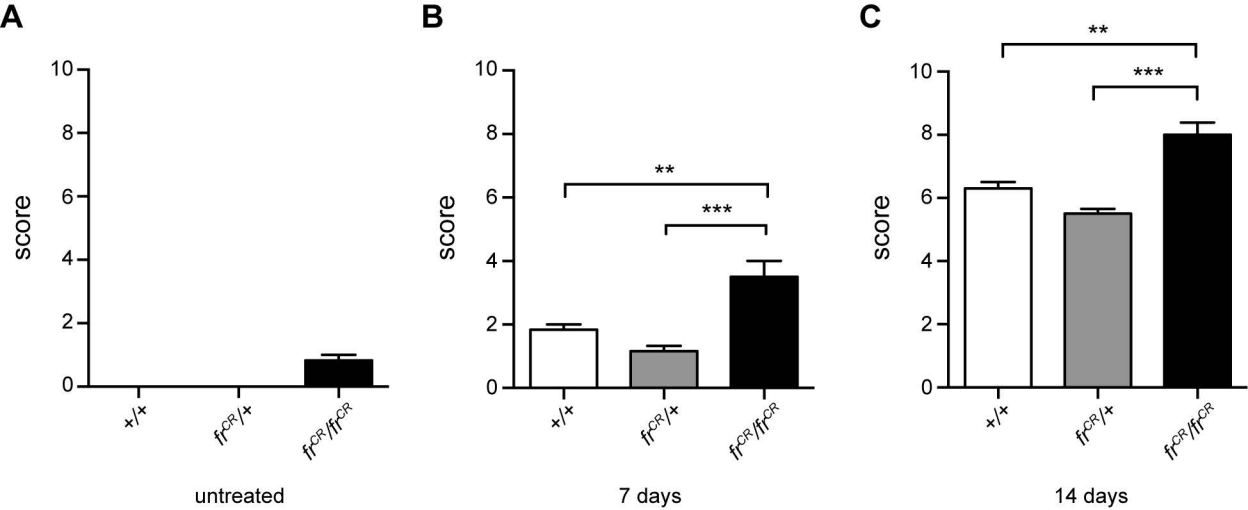
A
B
C
score
10
8
6
4
2
0
**
***
+/+
ff^CR/+
ff^CR/ff^CR
untreated
7 days
14 days

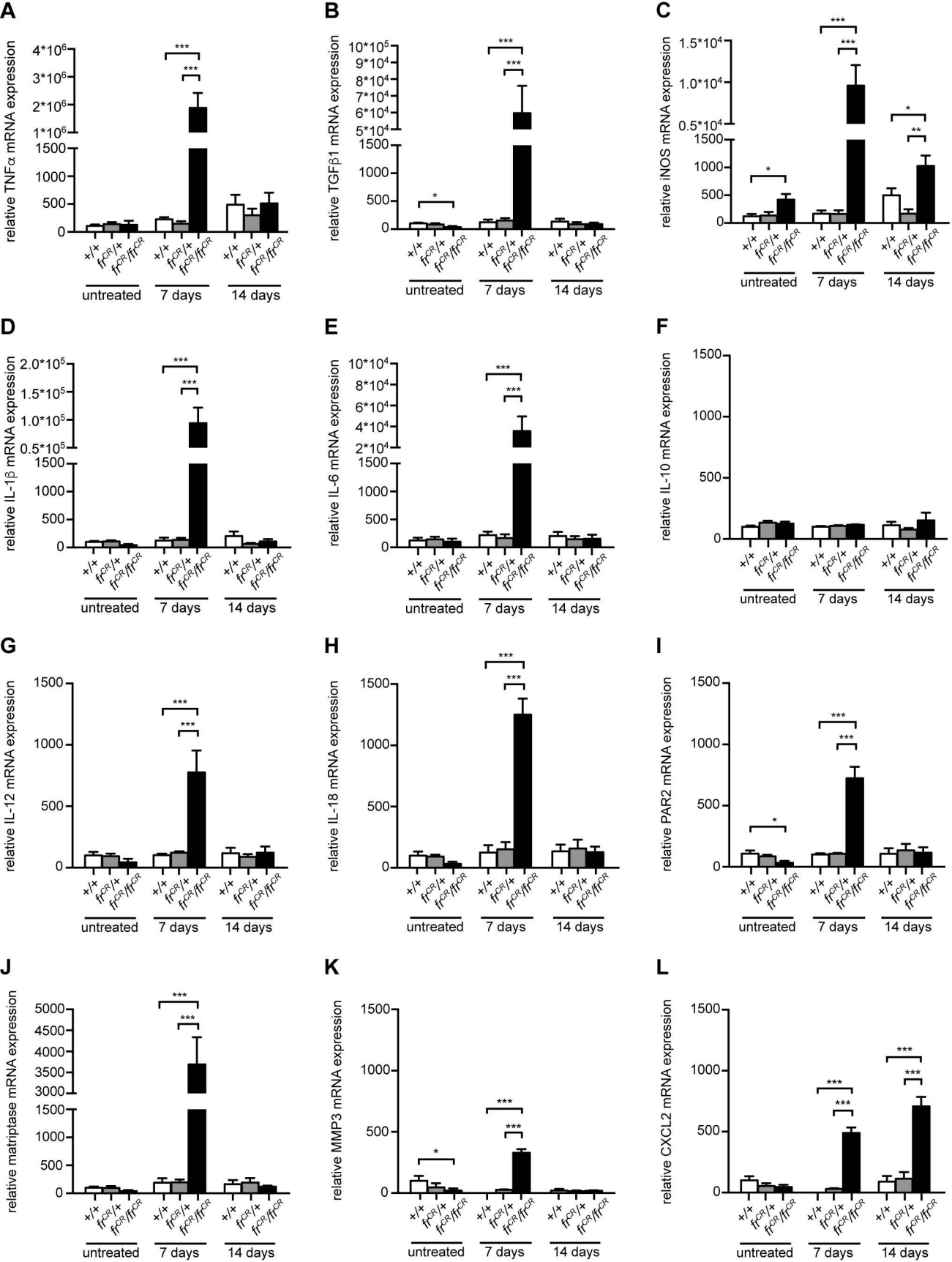
A
relative TNFα mRNA expression
B
relative TGFβ1 mRNA expression
C
relative iNOS mRNA expression
D
relative IL-1β mRNA expression
E
relative IL-6 mRNA expression
F
relative IL-10 mRNA expression
G
relative IL-12 mRNA expression
H
relative IL-18 mRNA expression
I
relative PAR2 mRNA expression
J
relative matriptase mRNA expression
K
relative MMP3 mRNA expression
L
relative CXCL2 mRNA expression
+/+
fr^CR/+
fr^CR/fr^CR
untreated
7 days
14 days

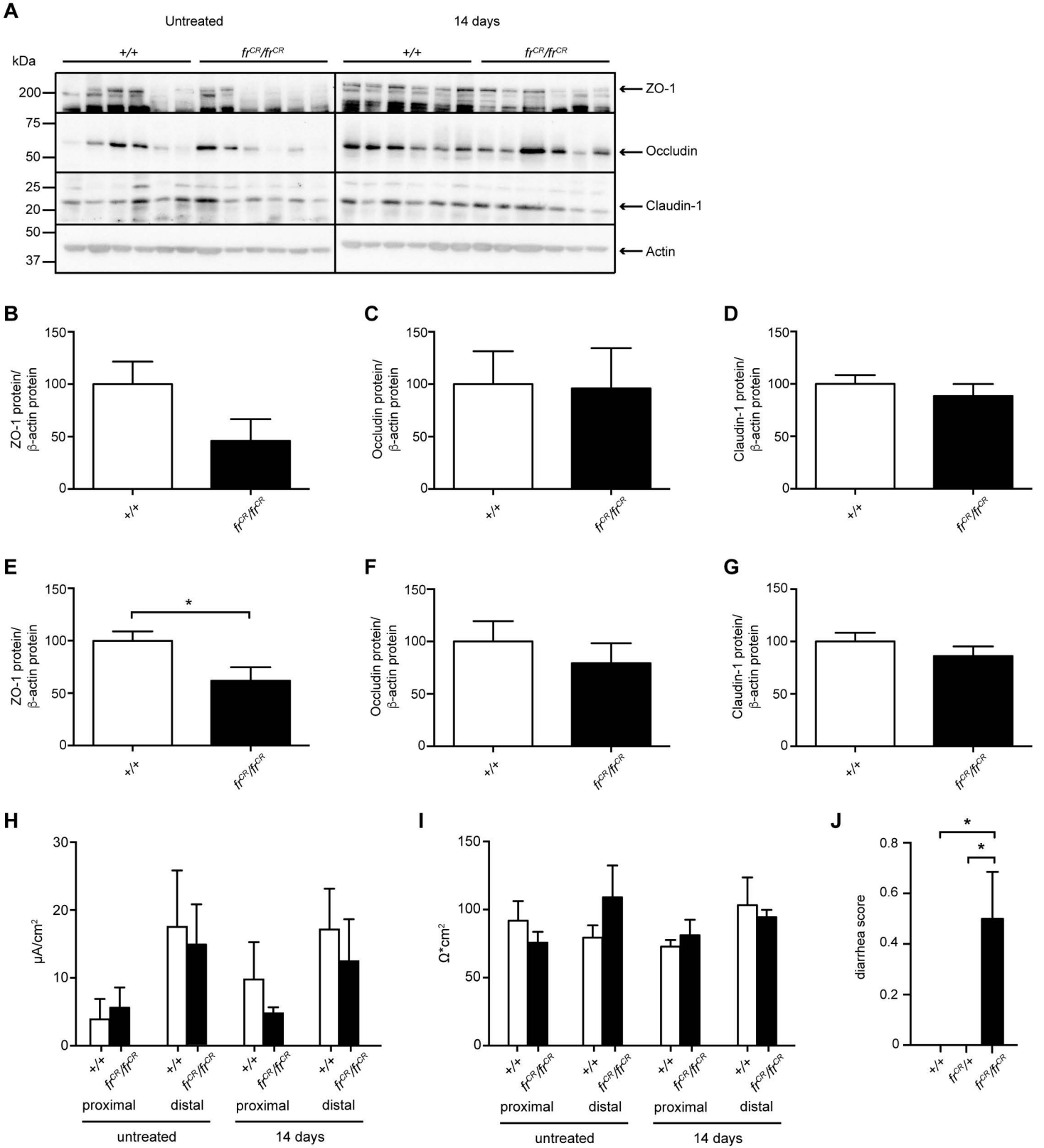
A
Untreated
14 days
+/+
fr^CR/fr^CR
+/+
fr^CR/fr^CR
kDa
200
75
50
25
20
50
37
ZO-1
Occludin
Claudin-1
Actin
B
ZO-1 protein/ β-actin protein
C
Occludin protein/ β-actin protein
D
Claudin-1 protein/ β-actin protein
E
ZO-1 protein/ β-actin protein
*
F
Occludin protein/ β-actin protein
G
Claudin-1 protein/ β-actin protein
H
µA/cm²
proximal
distal
proximal
distal
untreated
14 days
I
Ω*cm²
proximal
distal
proximal
distal
untreated
14 days
J
diarrhea score
*
*
+/+
fr^CR/+
fr^CR/fr^CR

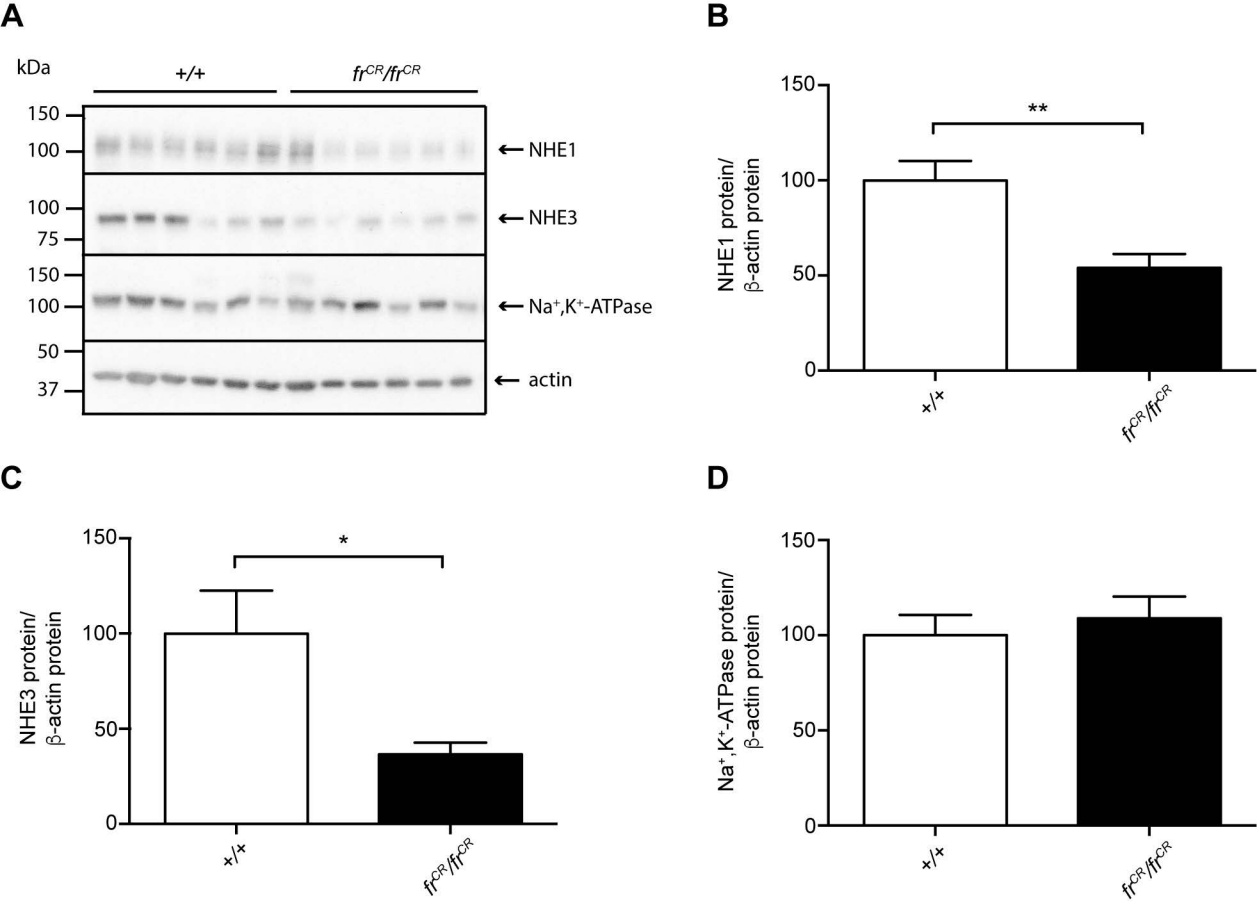
A
kDa
+/+
fr^CR/fr^CR
150
100
NHE1
100
75
NHE3
150
100
Na+,K+-ATPase
50
37
actin
B
NHE1 protein/
β-actin protein
150
100
50
0
**
+/+
fr^CR/fr^CR
C
NHE3 protein/
β-actin protein
150
100
50
0
*
+/+
fr^CR/fr^CR
D
Na+,K+-ATPase protein/
β-actin protein
150
100
50
0
+/+
fr^CR/fr^CR

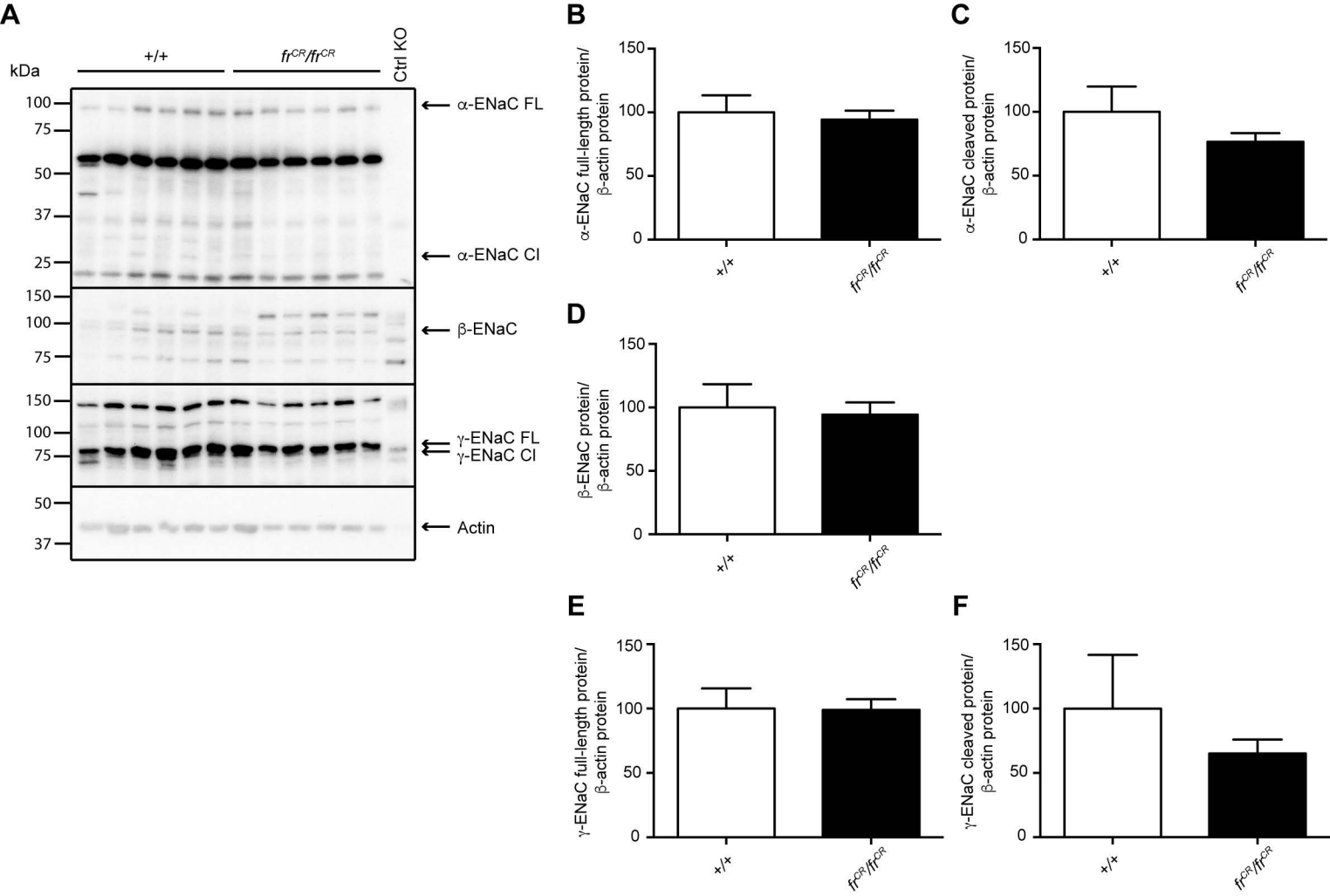
A
kDa
+/+
fr^CR/fr^CR
Ctrl KO
100
75
50
37
25
150
100
75
150
100
75
50
37
α-ENaC FL
α-ENaC Cl
β-ENaC
γ-ENaC FL
γ-ENaC Cl
Actin
B
α-ENaC full-length protein/ β-actin protein
C
α-ENaC cleaved protein/ β-actin protein
D
β-ENaC protein/ β-actin protein
E
γ-ENaC full-length protein/ β-actin protein
F
γ-ENaC cleaved protein/ β-actin protein
150
100
50
0
+/+
fr^CR/fr^CR

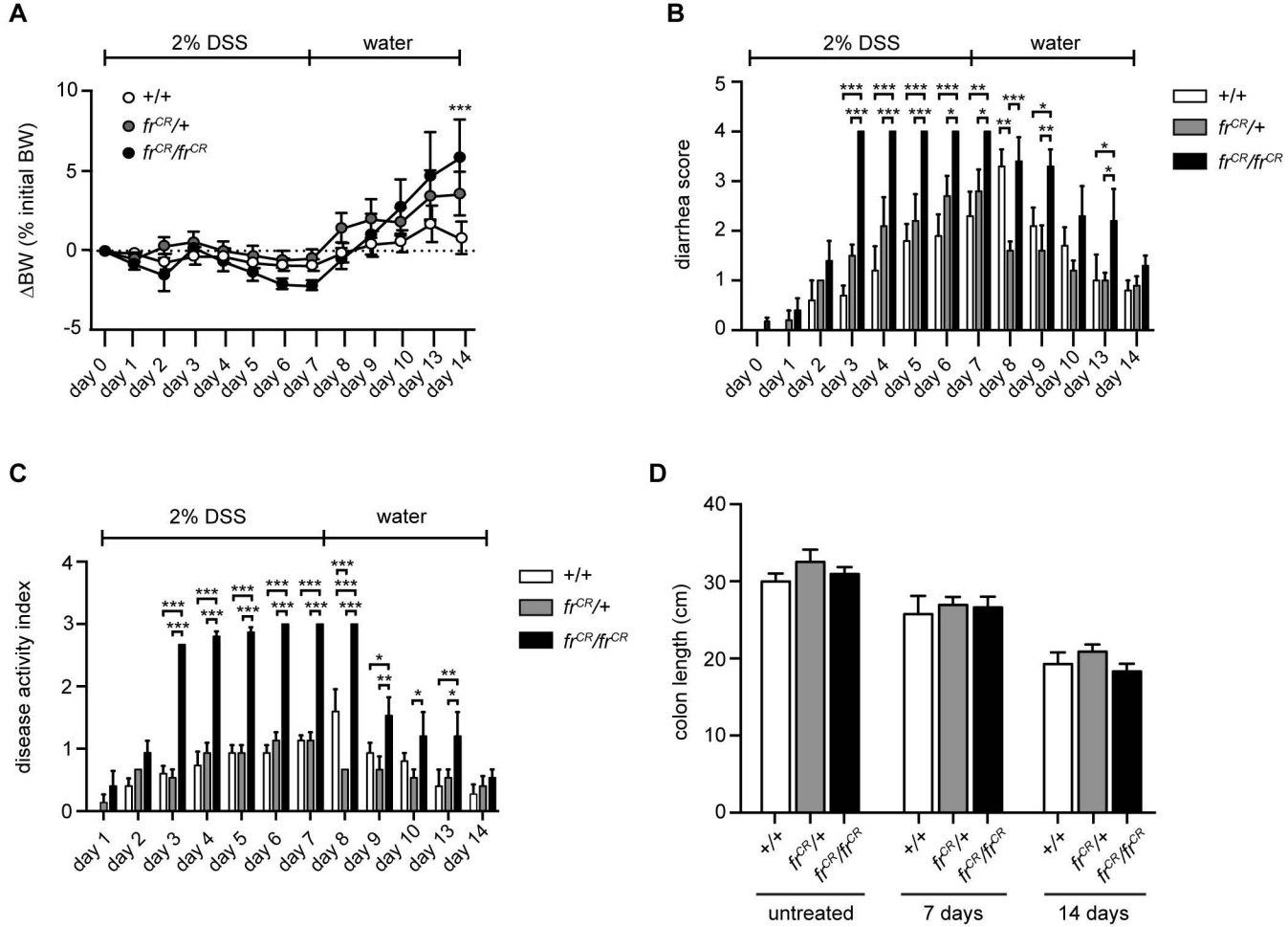
A
2% DSS
water
+/+
fr^CR/+
fr^CR/fr^CR
ΔBW (% initial BW)
day 0
day 1
day 2
day 3
day 4
day 5
day 6
day 7
day 8
day 9
day 10
day 13
day 14
B
diarrhea score
C
disease activity index
D
colon length (cm)
untreated
7 days
14 days

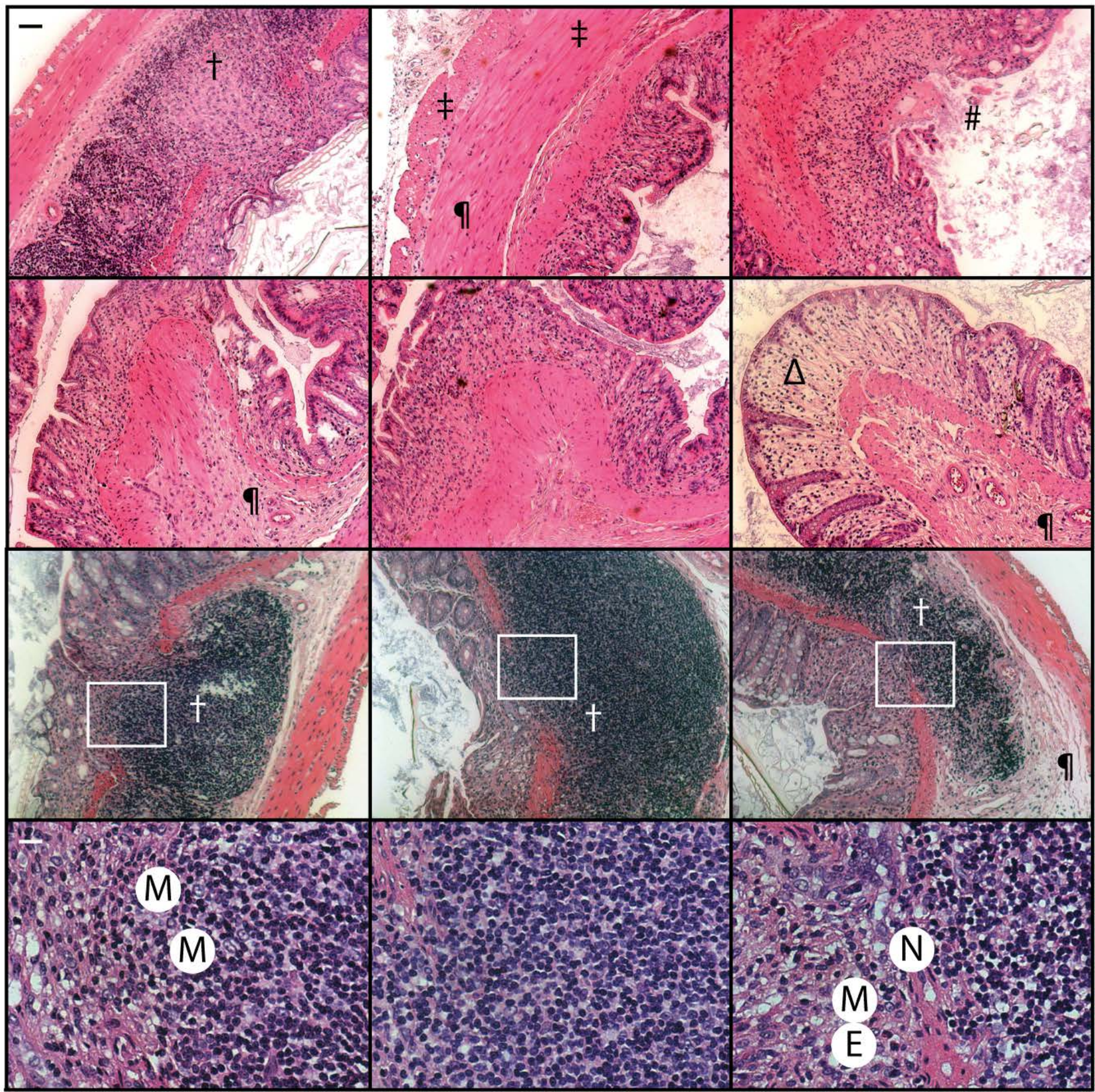
+/+
fr^CR/+
fr^CR/fr^CR
10X
10X
10X
40X
M
M
N
M
E

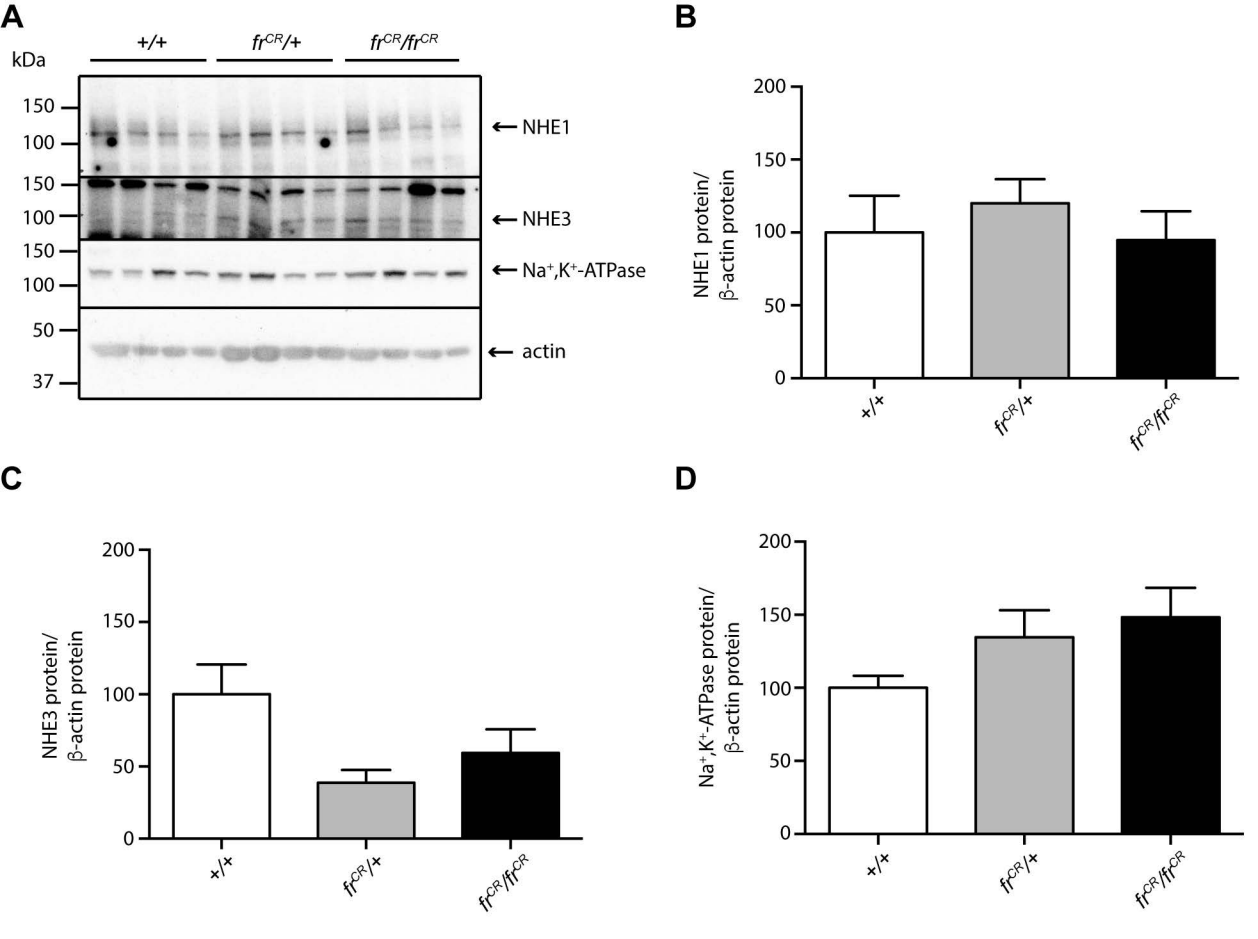
A
+/+
fr^CR/+
fr^CR/fr^CR
kDa
150
100
150
100
150
100
50
37
← NHE1
← NHE3
← Na+,K+-ATPase
← actin
B
NHE1 protein/
β-actin protein
200
150
100
50
0
+/+
fr^CR/+
fr^CR/fr^CR
C
NHE3 protein/
β-actin protein
200
150
100
50
0
+/+
fr^CR/+
fr^CR/fr^CR
D
Na+,K+-ATPase protein/
β-actin protein
200
150
100
50
0
+/+
fr^CR/+
fr^CR/fr^CR

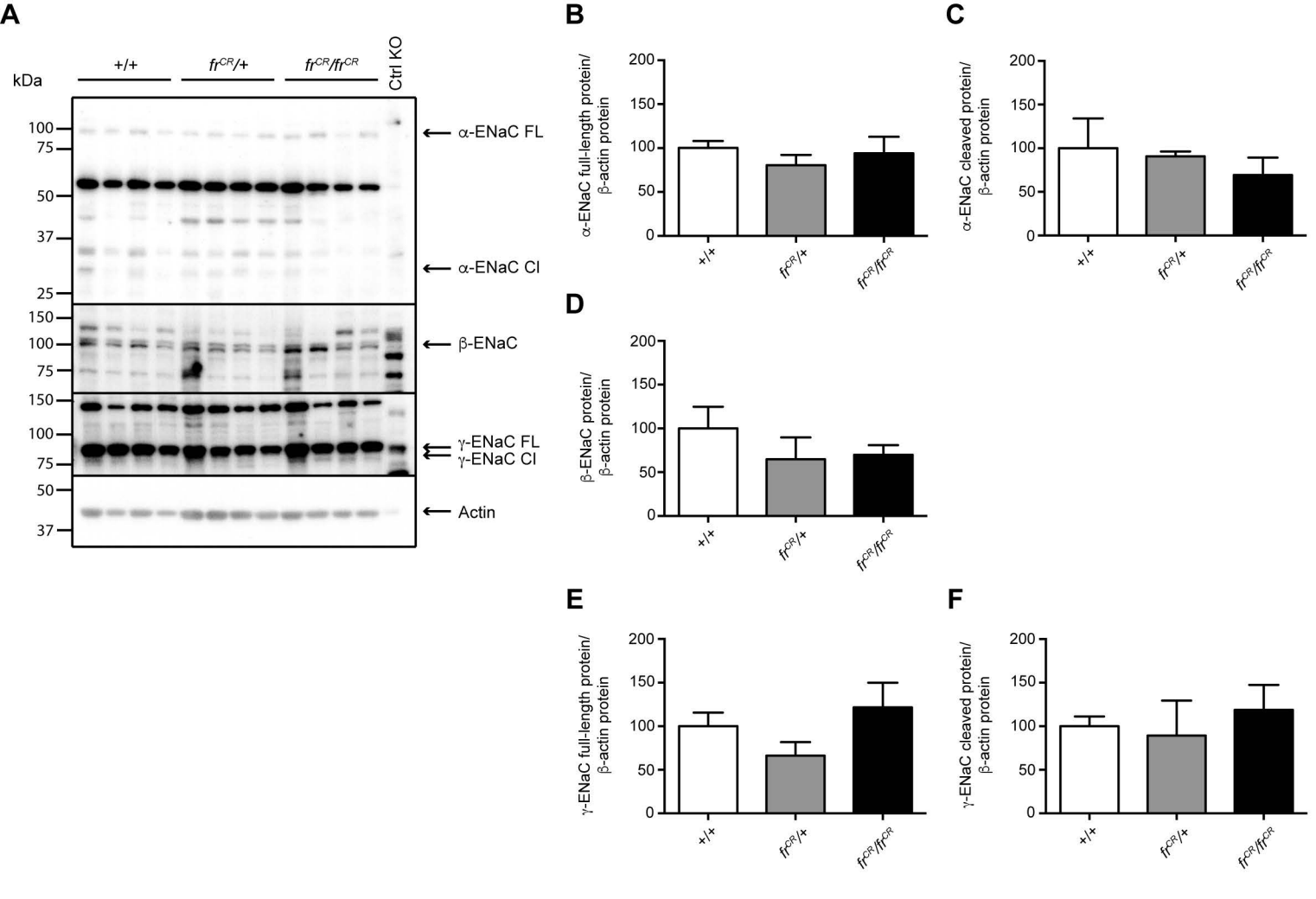
A
+/+
fr^CR/+
fr^CR/fr^CR
Ctrl KO
kDa
100
75
50
37
25
150
100
75
150
100
75
50
37
α-ENaC FL
α-ENaC Cl
β-ENaC
γ-ENaC FL
γ-ENaC Cl
Actin
B
α-ENaC full-length protein/ β-actin protein
200
150
100
50
0
+/+
fr^CR/+
fr^CR/fr^CR
C
α-ENaC cleaved protein/ β-actin protein
D
β-ENaC protein/ β-actin protein
E
γ-ENaC full-length protein/ β-actin protein
F
γ-ENaC cleaved protein/ β-actin protein

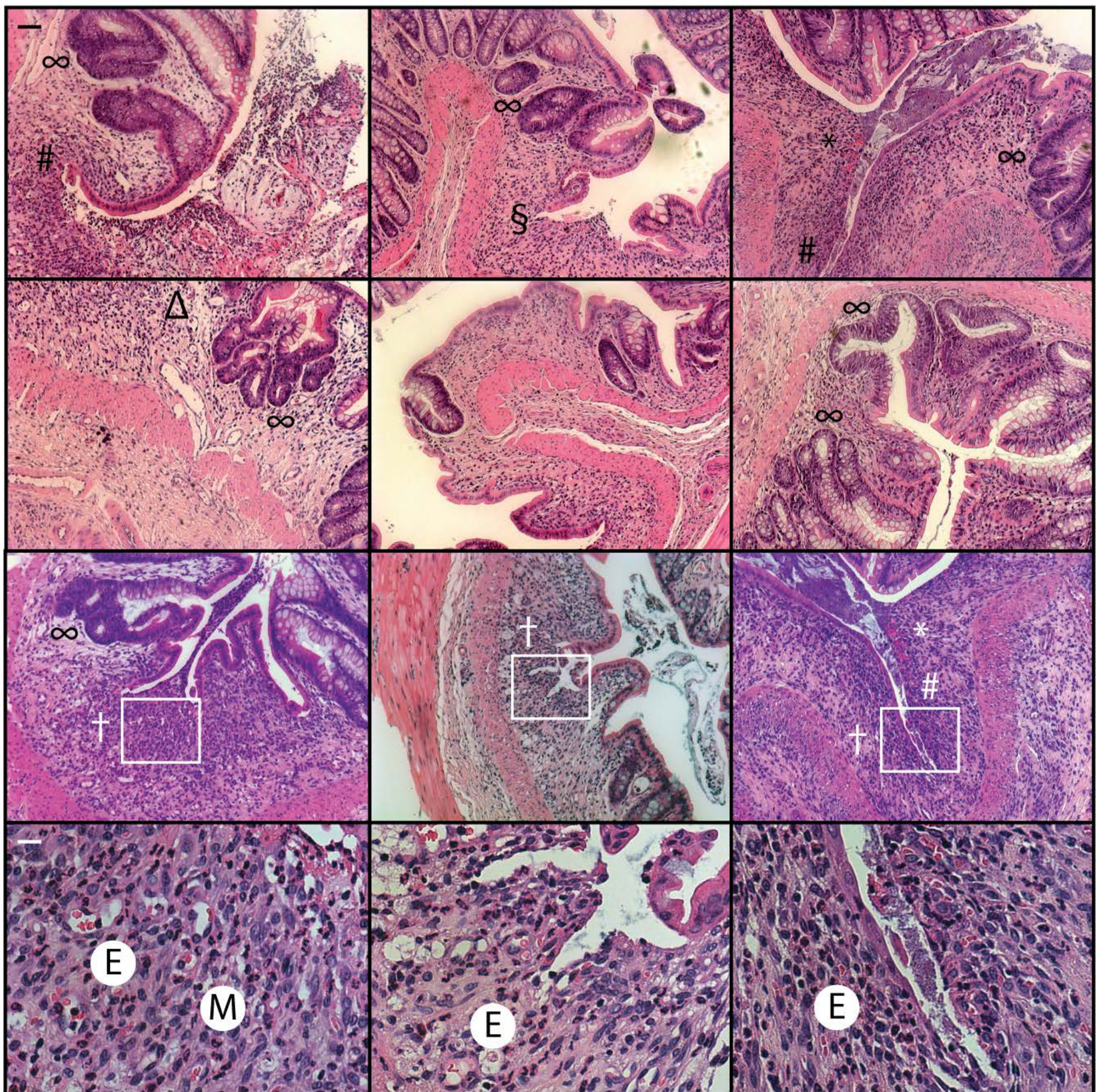
+/+
fr^CR/+
fr^CR/fr^CR
10X
10X
10X
40X
E
M
E
E